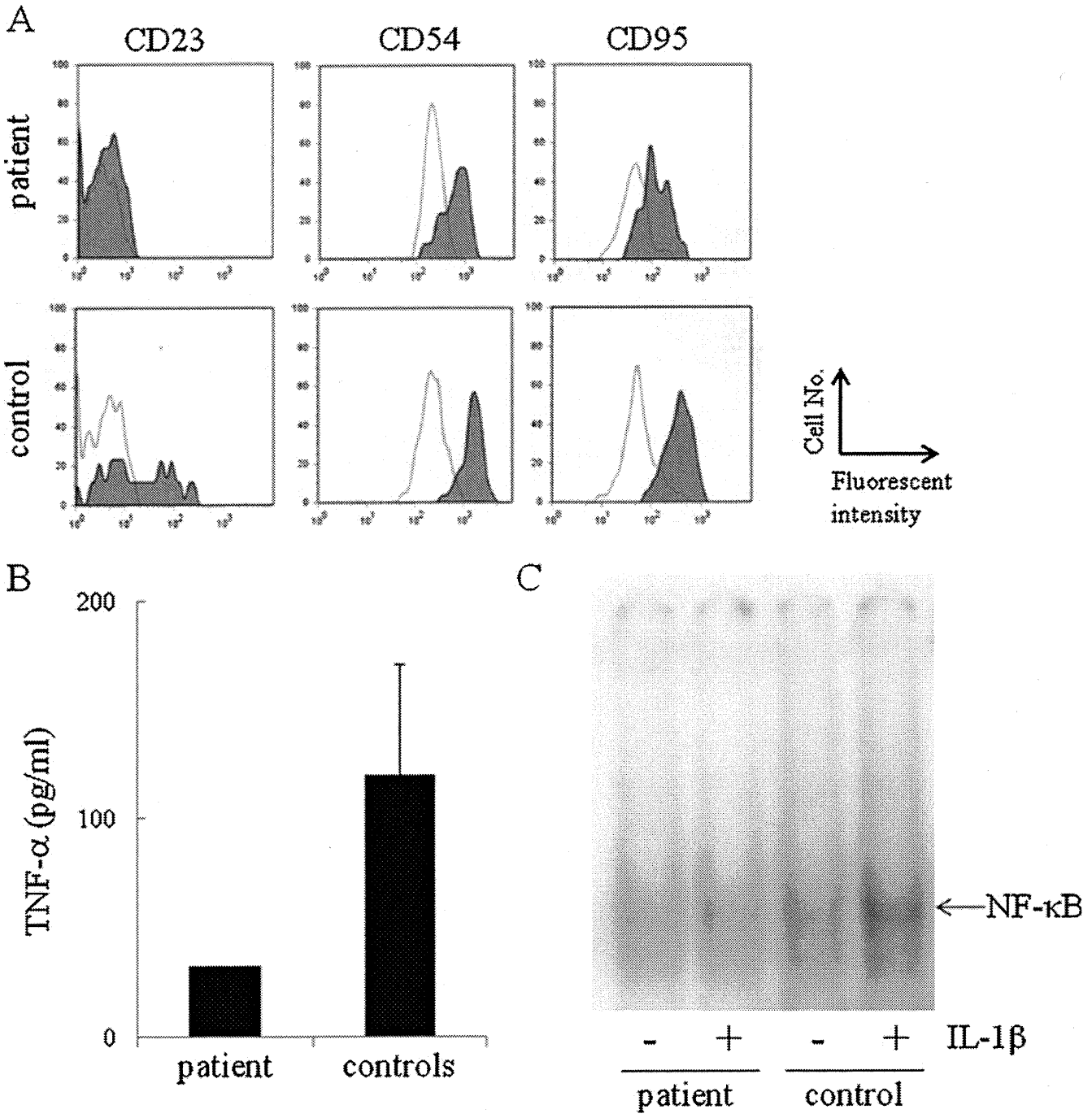

Fig. 4 Analysis of functional activity via NEMO. **a** Expression of CD23, CD54, and CD95, the surface markers of activated B cells, was measured using flow cytometry. PBMCs from the patient and healthy controls were treated with (*shaded histograms*) or without (*open histograms*) CD40L. **b** TNF-α production in response to LPS by $CD14^+$ cells was measured by Luminex. Data from the healthy subjects are represented as mean ± SD (n=4). **c** The NF-κB DNA-binding ability in response to IL-1β was measured by electrophoretic mobility shift assay. EBV-B cells from the patient showed a lower level of DNA-binding ability than healthy controls

collection in the patient with a 1056−1 G>A mutation. Curiously, however, there is a difference between the expression of WT-NEMO protein and the frequency of WT-NEMO mRNA in our patient. Although the frequency of WT-NEMO mRNA observed in the patient in our splicing assay was approximately 30% of all splice transcripts, expression of NEMO protein from the patient was only 12.5% that of WT levels. We suspect that the influence of nonsense-mediated RNA decay can explain this inconsistency between WT-NEMO expression at the mRNA and protein level. Some abnormally spliced forms of NEMO, such as 64-NEMO, result in premature stop codon. These

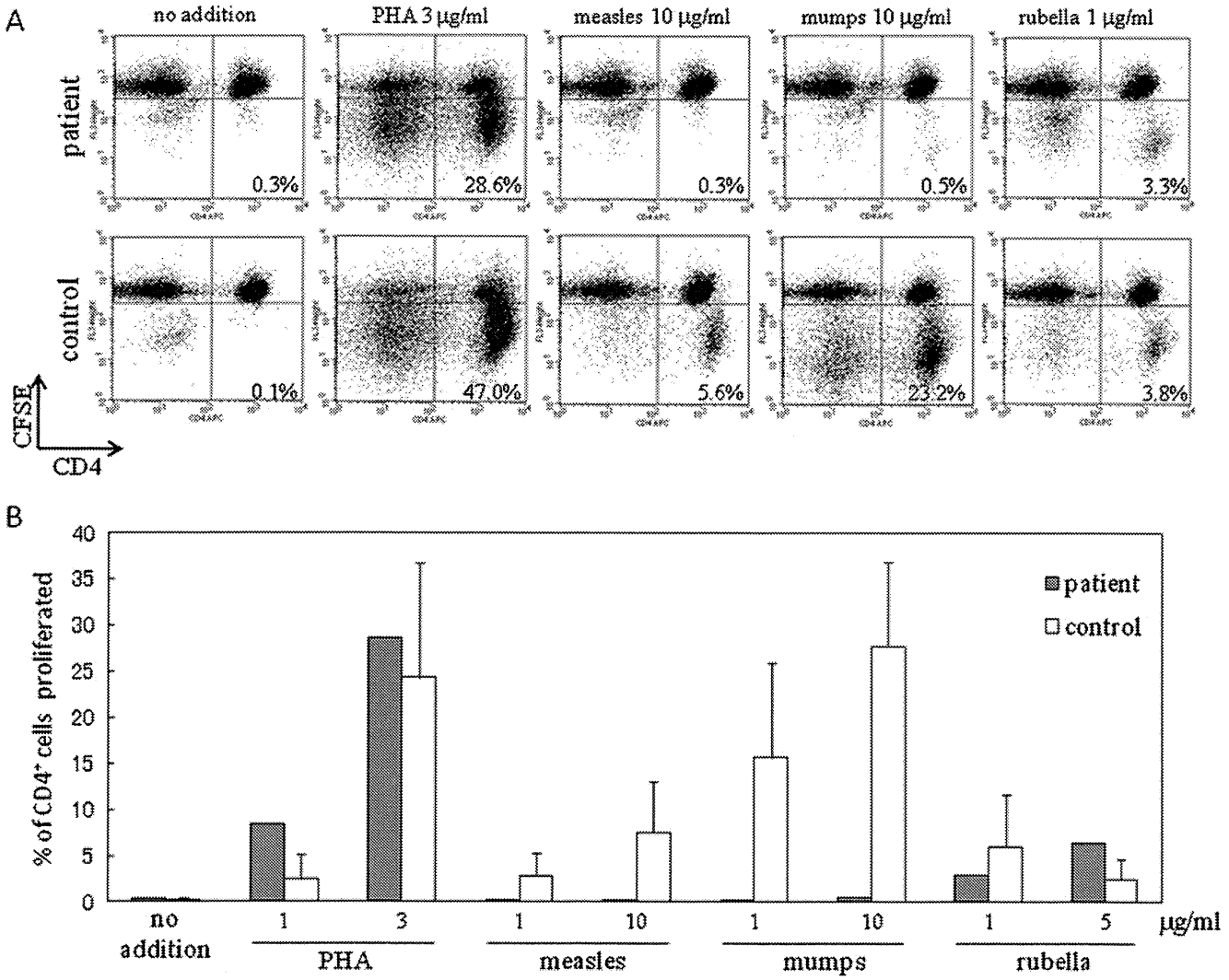

Fig. 5 CFSE analysis of the response of $CD4^+$ cells to PHA and various viruses. **a** Representative FACS figures from the patient and healthy subjects are shown. The *lower-right quadrant* of the FACS profile indicates the proportion of $CD4^+$ T cells that had undergone division in response to the indicated stimuli. **b** Summary of the percentage of proliferating $CD4^+$ T cells is shown. The data in the *white columns* represent the mean ± SD of five healthy subjects. Although $CD4^+$ T cells from the patient proliferated in response to the rubella virus, few divided cells were observed upon stimulation with the measles or mumps viruses

products are predicted to be susceptible to nonsense-mediated RNA decay. Therefore, although the splicing assay in this study is an effective way to detect variously spliced transcripts derived from the 769−1 G>C mutation, it may overestimate the proportion of in-frame transcripts which include WT-NEMO.

The other possibility to explain the existence of both WT and mutant mRNAs is germ-line or reversion mosaicism of WT and mutant NEMO-containing cells, as has previously been reported in patients with immunological disorders [28–31]. Furthermore, a reversion mosaicism has been identified in one patient with XL-ED-ID [12]. This patient exhibited NEMO protein expression that varied among cell lineages. Two types of NEMO-expressing cells, NEMO high and NEMO low, were observed by flow cytometric analysis. However, the pattern of NEMO expression did not differ among the lineages in our current study (Fig. 3a). In addition, we did not identify the WT-NEMO sequence from Sanger sequence using genomic DNA extracted from peripheral blood leukocytes or buccal mucosa from the patient (Fig. 1a). Taken together, although we could not completely exclude the possibility of low frequency mosaicism, we presume that normal NEMO mRNAs are derived from leakage through the splice-site mutation that may give rise to XL-ED-ID.

The levels of NEMO protein expression decreased markedly, and the functional activity via NEMO in response to various stimuli were impaired in our patient. Recently, Mooster et al. reported a patient with immunodeficiency caused by a splice-site mutation in the 5′ UTR of the

IKBKG [20]. This patient also showed decreased expression of the NEMO protein, thus resulting in reduced NF-κB activity. In addition, the authors proposed that inadequate levels of normal NEMO protein played a role in the molecular pathogenesis of this patient. Similarly, decreased expression of NEMO protein was also suspected to have played an important role in the clinical manifestations of our patient. However, in contrast to our patient, neither the patients with 1056−1 G>C nor 5′ UTR mutation that demonstrated a residual expression of WT-NEMO presented with ectodermal dysplasia. Further studies will therefore be required to elucidate the factor that is associated with the development of the ectodermal phenotype.

$CD4^+$ T cells from the patient exhibit impaired proliferation in response to measles and mumps viruses. On the other hand, normal proliferation was observed upon stimulation with the rubella virus. To our knowledge, this is the first study to clarify an impairment of T cell proliferation in response to viral infections by CSFE analysis in a patient with NEMO mutation. These results were completely consistent with the laboratory finding of specific antibody production against rubella, but not measles and mumps viruses. Furthermore, the impairment of antibody production against measles, but not rubella, was also observed in another patient with ED-ID carrying a D311E hypomorphic mutation in *NEMO* (Imai et al., in revision in J Clin Immunol). It is interesting to speculate how the impairment of the NEMO protein disturbs the response against measles. Generally, the first line of host defense against viral infection is the innate immune system [32]. Viral infections induce inflammatory reactions via induction of IFNs and via the activation of NF-κB. The activation of interferon regulatory factor-3 (IRF-3) plays an important role in the induction of IFNs against viral infections. IRF-3 recognizes the measles virus nucleocapsid and triggers the induction of interferon production. However, IRF-3 activation and IRF-3-dependent gene induction are abrogated in NEMO-deficient cells [33]. Indeed, impairment of TLR3-induced NF-κB- and IRF-3-dependent IFN induction has also been documented in a patient with NEMO mutation (Audry et al. J Allergy Clin Immunol. in press, reference number: YMAI 8998). In addition, the activation of NF-κB also plays a pivotal role in the host defense against measles. The measles virus phosphoprotein upregulates the ubiquitin-modifying enzyme A20, a negative feedback regulator of NF-κB, resulting in viral escape from the host immune system [34, 35]. Therefore, the impairments of acquired immunity against viral infections observed in the patient may be derived from an impairment of innate immunity caused by NEMO mutation. Further studies will therefore be required to confirm the clinical and cellular phenotype against viral infections in other patients with NEMO mutation.

Conclusion

The 769−1 G>C mutation was shown to cause a decrease in NF-κB activation through the decreased expression level of NEMO protein, thus resulting in the development of XL-ED-ID.

Acknowledgments This work was supported by a Grant-in-Aid for Young Scientist (B) No. 20790731 from Japan Society for the Promotion of Science. This work was also supported by the grants from the Japanese Ministry of Education, Culture, Sports, and Technology and grants from the Japanese Ministry of Health, Labor, and Welfare. We wish to thank the Analysis Center of Life Science, Hiroshima University for the use of their facilities. We also thank Natsuki Nabe and Yuki Takaoka for their valuable help with the reporter assay.

References

1. Doffinger R, Smahi A, Bessia C, Geissmann F, Feinberg J, Durandy A, et al. X-linked anhidrotic ectodermal dysplasia with immunodeficiency is caused by impaired NF-kappaB signaling. Nat Genet. 2001;27:277–85.
2. Fusco F, Pescatore A, Bal E, Ghoul A, Paciolla M, Lioi MB, et al. Alterations of the IKBKG locus and diseases: an update and a report of 13 novel mutations. Hum Mutat. 2008;29:595–604.
3. Puel A, Picard C, Ku CL, Smahi A, Casanova JL. Inherited disorders of NF-kappaB-mediated immunity in man. Curr Opin Immunol. 2004;16:34–41.
4. Courtois G, Smahi A, Israel A. NEMO/IKK gamma: linking NF-kappa B to human disease. Trends Mol Med. 2001;7:427–30.
5. Hanson EP, Monaco-Shawver L, Solt LA, Madge LA, Banerjee PP, May MJ, et al. Hypomorphic nuclear factor-kappaB essential modulator mutation database and reconstitution system identifies phenotypic and immunologic diversity. J Allergy Clin Immunol. 2008;122:1169–77.
6. Orange JS, Jain A, Ballas ZK, Schneider LC, Geha RS, Bonilla FA. The presentation and natural history of immunodeficiency caused by nuclear factor kappaB essential modulator mutation. J Allergy Clin Immunol. 2004;113:725–33.
7. Lee WI, Torgerson TR, Schumacher MJ, Yel L, Zhu Q, Ochs HD. Molecular analysis of a large cohort of patients with the hyper immunoglobulin M (IgM) syndrome. Blood. 2005;105:1881–90.
8. Filipe-Santos O, Bustamante J, Haverkamp MH, Vinolo E, Ku CL, Puel A, et al. X-linked susceptibility to mycobacteria is caused by mutations in NEMO impairing CD40-dependent IL-12 production. J Exp Med. 2006;203:1745–59.
9. Orange JS, Brodeur SR, Jain A, Bonilla FA, Schneider LC, Kretschmer R, et al. Deficient natural killer cell cytotoxicity in patients with IKK-gamma/NEMO mutations. J Clin Invest. 2002;109(11):1501–9.
10. Vinolo E, Sebban H, Chaffotte A, Israel A, Courtois G, Veron M, et al. A point mutation in NEMO associated with anhidrotic ectodermal dysplasia with immunodeficiency pathology results in destabilization of the oligomer and reduces lipopolysaccharide- and tumor necrosis factor-mediated NF-kappa B activation. J Biol Chem. 2006;281:6334–48.
11. Smahi A, Courtois G, Rabia SH, Doffinger R, Bodemer C, Munnich A, et al. The NF-kappaB signalling pathway in human diseases: from incontinentia pigmenti to ectodermal dysplasias and immune-deficiency syndromes. Hum Mol Genet. 2002;11:2371–5.

12. Nishikomori R, Akutagawa H, Maruyama K, Nakata-Hizume M, Ohmori K, Mizuno K, et al. X-linked ectodermal dysplasia and immunodeficiency caused by reversion mosaicism of NEMO reveals a critical role for NEMO in human T-cell development and/or survival. Blood. 2004;103:4565–72.
13. Puel A, Reichenbach J, Bustamante J, Ku CL, Feinberg J, Doffinger R, et al. The NEMO mutation creating the most-upstream premature stop codon is hypomorphic because of a reinitiation of translation. Am J Hum Genet. 2006;78:691–701.
14. Fazekas de St Groth B, Smith AL, Koh WP, Girgis L, Cook MC, Bertolino P. Carboxyfluorescein diacetate succinimidyl ester and the virgin lymphocyte: a marriage made in heaven. Immunol Cell Biol. 1999;77:530–8.
15. Lyons AB. Analysing cell division in vivo and in vitro using flow cytometric measurement of CFSE dye dilution. J Immunol Methods. 2000;243:147–54.
16. Mount SM. A catalogue of splice junction sequences. Nucleic Acids Res. 1982;10:459–72.
17. Mount SM. Genomic sequence, splicing, and gene annotation. Am J Hum Genet. 2000;67:788–92.
18. Jain A, Ma CA, Liu S, Brown M, Cohen J, Strober W. Specific missense mutations in NEMO result in hyper-IgM syndrome with hypohydrotic ectodermal dysplasia. Nat Immunol. 2001;2:223–8.
19. Jain A, Ma CA, Lopez-Granados E, Means G, Brady W, Orange JS, et al. Specific NEMO mutations impair CD40-mediated c-Rel activation and B cell terminal differentiation. J Clin Invest. 2004;114:1593–602.
20. Mooster JL, Cancrini C, Simonetti A, Rossi P, Di Matteo G, Romiti ML, et al. Immune deficiency caused by impaired expression of nuclear factor-kappaB essential modifier (NEMO) because of a mutation in the 5′ untranslated region of the NEMO gene. J Allergy Clin Immunol. 2010;126:127–32.
21. Kouskoff V, Nemazee D. Role of receptor editing and revision in shaping the B and T lymphocyte repertoire. Life Sci. 2001;69:1105–13.
22. Souto-Carneiro MM, Fritsch R, Sepulveda N, Lagareiro MJ, Morgado N, Longo NS, et al. The NF-kappaB canonical pathway is involved in the control of the exonucleolytic processing of coding ends during V(D)J recombination. J Immunol. 2008;180:1040–9.
23. Munier CM, Zaunders JJ, Ip S, Cooper DA, Kelleher AD. A culture amplified multi-parametric intracellular cytokine assay (CAMP-ICC) for enhanced detection of antigen specific T-cell responses. J Immunol Methods. 2009;345:1–16.
24. Arredondo-Vega FX, Santisteban I, Kelly S, Schlossman CM, Umetsu DT, Hershfield MS. Correct splicing despite mutation of the invariant first nucleotide of a 5′ splice site: a possible basis for disparate clinical phenotypes in siblings with adenosine deaminase deficiency. Am J Hum Genet. 1994;54:820–30.
25. Krawczak M, Reiss J, Cooper DN. The mutational spectrum of single base-pair substitutions in mRNA splice junctions of human genes: causes and consequences. Hum Genet. 1992;90:41–54.
26. Seyama K, Nonoyama S, Gangsaas I, Hollenbaugh D, Pabst HF, Aruffo A, et al. Mutations of the CD40 ligand gene and its effect on CD40 ligand expression in patients with X-linked hyper IgM syndrome. Blood. 1998;92:2421–34.
27. Orange JS, Levy O, Brodeur SR, Krzewski K, Roy RM, Niemela JE, et al. Human nuclear factor kappa B essential modulator mutation can result in immunodeficiency without ectodermal dysplasia. J Allergy Clin Immunol. 2004;114:650–6.
28. Arveiler B, de Saint-Basile G, Fischer A, Griscelli C, Mandel JL. Germ-line mosaicism simulates genetic heterogeneity in Wiskott–Aldrich syndrome. Am J Hum Genet. 1990;46:906–11.
29. Hirschhorn R, Yang DR, Puck JM, Huie ML, Jiang CK, Kurlandsky LE. Spontaneous in vivo reversion to normal of an inherited mutation in a patient with adenosine deaminase deficiency. Nat Genet. 1996;13:290–5.
30. Wada T, Schurman SH, Otsu M, Garabedian EK, Ochs HD, Nelson DL, et al. Somatic mosaicism in Wiskott–Aldrich syndrome suggests in vivo reversion by a DNA slippage mechanism. Proc Natl Acad Sci U S A. 2001;98:8697–702.
31. Stephan V, Wahn V, Le Deist F, Dirksen U, Broker B, Muller-Fleckenstein I, et al. Atypical X-linked severe combined immunodeficiency due to possible spontaneous reversion of the genetic defect in T cells. N Engl J Med. 1996;335:1563–7.
32. Yokota S, Okabayashi T, Fujii N. The battle between virus and host: modulation of Toll-like receptor signaling pathways by virus infection. Mediators Inflamm. 2010;2010:184328.
33. Zhao T, Yang L, Sun Q, Arguello M, Ballard DW, Hiscott J, et al. The NEMO adaptor bridges the nuclear factor-kappaB and interferon regulatory factor signaling pathways. Nat Immunol. 2007;8:592–600.
34. Indoh T, Yokota S, Okabayashi T, Yokosawa N, Fujii N. Suppression of NF-kappaB and AP-1 activation in monocytic cells persistently infected with measles virus. Virology. 2007;361:294–303.
35. Yokota S, Okabayashi T, Yokosawa N, Fujii N. Measles virus P protein suppresses Toll-like receptor signal through up-regulation of ubiquitin-modifying enzyme A20. FASEB J. 2008;22:74–83.

Published July 4, 2011

JEM

Article

Gain-of-function human *STAT1* mutations impair IL-17 immunity and underlie chronic mucocutaneous candidiasis

Luyan Liu,[1] Satoshi Okada,[2] Xiao-Fei Kong,[2] Alexandra Y. Kreins,[2] Sophie Cypowyj,[2] Avinash Abhyankar,[2] Julie Toubiana,[3] Yuval Itan,[2] Magali Audry,[2] Patrick Nitschke,[4] Cécile Masson,[4] Beata Toth,[9] Jérome Flatot,[1] Mélanie Migaud,[1] Maya Chrabieh,[1] Tatiana Kochetkov,[2] Alexandre Bolze,[1,2] Alessandro Borghesi,[1] Antoine Toulon,[5] Julia Hiller,[10] Stefanie Eyerich,[10] Kilian Eyerich,[10,11] Vera Gulácsy,[9] Ludmyla Chernyshova,[12] Viktor Chernyshov,[13] Anastasia Bondarenko,[12] Rosa María Cortés Grimaldo,[14] Lizbeth Blancas-Galicia,[15] Ileana Maria Madrigal Beas,[14] Joachim Roesler,[16] Klaus Magdorf,[17] Dan Engelhard,[18] Caroline Thumerelle,[19] Pierre-Régis Burgel,[20] Miriam Hoernes,[21] Barbara Drexel,[21] Reinhard Seger,[21] Theresia Kusuma,[22] Annette F. Jansson,[22] Julie Sawalle-Belohradsky,[22] Bernd Belohradsky,[22] Emmanuelle Jouanguy,[1,2] Jacinta Bustamante,[1] Mélanie Bué,[23] Nathan Karin,[24] Gizi Wildbaum,[24] Christine Bodemer,[5] Olivier Lortholary,[6] Alain Fischer,[7] Stéphane Blanche,[7] Saleh Al-Muhsen,[24] Janine Reichenbach,[21] Masao Kobayashi,[26] Francisco Espinosa Rosales,[15] Carlos Torres Lozano,[14] Sara Sebnem Kilic,[27] Matias Oleastro,[28] Amos Etzioni,[24] Claudia Traidl-Hoffmann,[10,11] Ellen D. Renner,[22] Laurent Abel,[1,2] Capucine Picard,[1,6,8] László Maródi,[9] Stéphanie Boisson-Dupuis,[1,2] Anne Puel,[1] and Jean-Laurent Casanova[1,2,7,25]

[1]Laboratory of Human Genetics of Infectious Diseases, Necker Branch, Necker Medical School, Institut National de la Santé et de la Recherche Médicale U980 and University Paris Descartes, 75015 Paris, France
[2]St. Giles Laboratory of Human Genetics of Infectious Diseases, Rockefeller Branch, The Rockefeller University, New York, NY 10065
[3]Department of Pediatrics, [4]Bioinformatics Unit, [5]Department of Dermatology, [6]Department of Infectious Diseases, [7]Pediatric Hematology-Immunology Unit, and [8]Center for Immunodeficiency, Necker Hospital, AP-HP, and University Paris Descartes, 75015 Paris, France
[9]Department of Infectious and Pediatric Immunology, Medical and Health Science Center, University of Debrecen, 4032 Debrecen, Hungary
[10]Center for Allergy and Environment, Helmholtz Center/TUM, 80802 Munich, Germany
[11]Department of Dermatology, Technische Universitat, 80802 Munich, Germany
[12]Department of Pediatric Infectious Diseases and Clinical Immunology, National Medical Academy for Post-Graduate Education, 01024 Kiev, Ukraine
[13]Laboratory of Immunology, Institute of Pediatrics, Obstetrics, and Gynecology, National Academy of Medical Sciences, 01024 Kiev, Ukraine
[14]Allergy and Immunology Department, UMAE-HE-CMNO-IMMS, 44500 Guadalajara, Mexico
[15]National Institute of Pediatrics, 04530 Mexico City, Mexico
[16]Department of Pediatrics, University Hospital Carl Gustav Carus, 01307 Dresden, Germany
[17]Department of Pediatric Pneumology and Immunology, Charité Medical School of Berlin, 11117 Berlin, Germany
[18]Department of Pediatrics, Hadassah University Hospital, 91120 Jerusalem, Israel
[19]Pneumology and Allergology Unit, Hospital Jeanne de Flandres, 59037 Lille, France
[20]Pneumology and UPRES EA 2511, Hospital Cochin, AP-HP, 75014 Paris, France
[21]Division of Immunology, Hematology, and BMT, Children's Research Center, Children's Hospital, University of Zurich, 8032 Zurich, Switzerland
[22]University Children's Hospital at Dr. von Haunersches Kinderspital, Ludwig Maximilian University, 80337 Munich, Germany
[23]University Hospital Center of Brest, 29609 Brest, France
[24]Rappaport Faculty of Medicine, Technion, 31096 Haifa, Israel.
[25]Prince Naif Center for Immunology Research, Department of Pediatrics, College of Medicine, King Saud University, Riyadh, 11461Saudi Arabia
[26]Department of Pediatrics, Hiroshima University Graduate School of Biomedical Sciences, 739-8511 Hiroshima, Japan
[27]Department of Pediatrics, Uludag University School of Medicine, 16059 Bursa, Turkey
[28]National Children's Hospital Prof. Dr. Juan P. Garrahan, 12049 Buenos Aires, Argentina

L. Liu, S. Okada, X.-F. Kong, A.Y. Kreins, and S. Cypowyj contributed equally to this paper.
A. Abhyankar, J. Toubiana, Y. Itan, M. Audry, P. Nitschke, C. Masson, and B. Toth contributed equally to this paper.
S. Al-Muhsen, J. Reichenbach, M. Kobayashi, F. Espinoza Rosales, C. Torres Lozano, S. Sebnem Kilic, M. Oleastro, A. Etzioni, C. Traidl-Hoffmann, E.D. Renner, L. Abel, and C. Picard contributed equally to this paper.
L. Maródi, S. Boisson-Dupuis, A. Puel, and J.-L. Casanova contributed equally to this paper.

CORRESPONDENCE
Anne Puel:
anne.puel@inserm.fr
OR
Jean-Laurent Casanova:
jean-laurent.casanova@rockefeller.edu

Abbreviations used: AD, autosomal dominant; AR, autosomal recessive; CMC, chronic mucocutaneous candidiasis; CMCD, CMC disease; EMSA, electrophoretic mobility shift assay; GAS, γ-activated sequence; ISRE, IFN-stimulated response element; MSMD, Mendelian susceptibility to mycobacterial disease; WB, Western blotting.

The Rockefeller University Press $30.00
J. Exp. Med. Vol. 208 No. 8 1635-1648
www.jem.org/cgi/doi/10.1084/jem.20110958

Supplemental Material can be found at:
http://jem.rupress.org/content/suppl/2011/07/03/jem.20110958.DC1.html

Published July 4, 2011

JEM

Chronic mucocutaneous candidiasis disease (CMCD) may be caused by autosomal dominant (AD) IL-17F deficiency or autosomal recessive (AR) IL-17RA deficiency. Here, using whole-exome sequencing, we identified heterozygous germline mutations in *STAT1* in 47 patients from 20 kindreds with AD CMCD. Previously described heterozygous *STAT1* mutant alleles are loss-of-function and cause AD predisposition to mycobacterial disease caused by impaired STAT1-dependent cellular responses to IFN-γ. Other loss-of-function *STAT1* alleles cause AR predisposition to intracellular bacterial and viral diseases, caused by impaired STAT1-dependent responses to IFN-α/β, IFN-γ, IFN-λ, and IL-27. In contrast, the 12 AD CMCD-inducing *STAT1* mutant alleles described here are gain-of-function and increase STAT1-dependent cellular responses to these cytokines, and to cytokines that predominantly activate STAT3, such as IL-6 and IL-21. All of these mutations affect the coiled-coil domain and impair the nuclear dephosphorylation of activated STAT1, accounting for their gain-of-function and dominance. Stronger cellular responses to the STAT1-dependent IL-17 inhibitors IFN-α/β, IFN-γ, and IL-27, and stronger STAT1 activation in response to the STAT3-dependent IL-17 inducers IL-6 and IL-21, hinder the development of T cells producing IL-17A, IL-17F, and IL-22. Gain-of-function *STAT1* alleles therefore cause AD CMCD by impairing IL-17 immunity.

Chronic mucocutaneous candidiasis (CMC) is characterized by persistent or recurrent disease of the nails, skin, oral, or genital mucosae caused by *Candida albicans* (Puel et al., 2010b). CMC may be caused by various inborn errors of immunity. CMC is one of a multitude of infectious diseases observed in patients with broad and profound T cell deficiencies. In contrast, patients with the autosomal dominant (AD) hyper IgE syndrome, caused by dominant-negative mutations of *STAT3*, are susceptible principally to CMC and staphylococcal diseases of the lungs and skin (Minegishi, 2009). These patients have very low proportions of circulating IL-17A– and IL-22–producing T cells, probably because of impaired responses to IL-6, IL-21, and/or IL-23 (de Beaucoudrey et al., 2008; Ma et al., 2008; Milner et al., 2008; Renner et al., 2008; Minegishi et al., 2009). Patients with autosomal recessive (AR) IL-12p40 or IL-12Rβ1 deficiency suffer from Mendelian susceptibility to mycobacterial disease (MSMD) and occasionally develop mild CMC (Filipe-Santos et al., 2006; de Beaucoudrey et al., 2010). Some have low proportions of IL-17A– and IL-22–producing T cells, presumably because of the abolition of IL-23 responses (de Beaucoudrey et al., 2008, 2010). The proportion of IL-17A–producing T cells was also found to be low in a family with AR CARD9 deficiency, dermatophytosis, invasive candidiasis, and CMC (Glocker et al., 2009). Finally, CMC is the only infection in patients with autoimmune polyendocrinopathy syndrome type 1, who have high titers of neutralizing autoantibodies against IL-17A, IL-17F, and IL-22 (Kisand et al., 2010; Puel et al., 2010a). Thus, regardless of the underlying illness, CMC pathogenesis apparently involves the impairment of IL-17A, IL-17F, and IL-22 immunity (Puel et al., 2010b).

The pathogenesis of CMC was eventually deciphered through investigations of patients with CMC disease (CMCD), in which CMC is isolated, with no other infectious or autoimmune signs (Kirkpatrick, 2001; Puel et al., 2010b). The definition of CMCD is not absolute, as illustrated in some patients by cutaneous staphylococcal disease, which is milder than that in patients with AD hyper IgE syndrome (Herrod, 1990), or by autoimmune features affecting the thyroid in particular, although fewer such features are observed than in patients with autoimmune polyendocrinopathy syndrome type 1 (Atkinson et al., 2001). It is unclear whether CMCD, with these or other manifestations (Shama and Kirkpatrick, 1980; Bentur et al., 1991; Germain et al., 1994), is immunologically and genetically related to pure CMCD. Low proportions of IL-17A–producing T cells have been documented in five patients with CMCD (Eyerich et al., 2008). Moreover, a candidate gene approach centered on IL-17 immunity recently revealed the first genetic etiologies of pure CMCD. In a consanguineous family from Morocco, a child with CMCD was found to display AR complete IL-17RA deficiency (Puel et al., 2011). His leukocytes and fibroblasts did not respond to IL-17A or IL-17F homodimers, or to IL-17A/F heterodimers. Four patients from an Argentinean family were shown to harbor dominant-negative mutations in the *IL17F* gene (Puel et al., 2011). Mutated IL-17F–containing homodimers and heterodimers were produced in normal amounts but were not biologically active, as they were unable to bind to the IL-17 receptor. Morbid mutations in *IL17RA* and *IL17F* demonstrated that CMCD could be caused by inborn errors of IL-17 immunity. However, no genetic etiology has yet been identified for most patients with CMCD. We set out to identify new genetic etiologies of CMCD through a recently developed genome-wide approach based on whole-exome sequencing (Alcaïs et al., 2010; Bolze et al., 2010; Byun et al., 2010; Ng et al., 2010).

RESULTS

We investigated one sporadic case and the probands from five multiplex kindreds with AD CMCD, by whole-exome sequencing. The annotated data were analyzed with sequence analysis software that had been developed in-house and made it possible to analyze and compare several exome sequences simultaneously. A hierarchy of candidate variations was generated by filtering out known polymorphisms reported in dbSNP and 1,000-genome databases. We also used our own database of 250 exomes to filter out unreported polymorphisms (Table S1). The only relevant gene displaying heterozygous variations in at least four of the six unrelated patients with AD CMCD was *STAT1* (Fig. 1, A and B, Kindreds A, B, G, and L; Table I; and Table S2). Three different *STAT1* mutations were found in four patients; they were confirmed by Sanger

Published July 4, 2011

sequencing and shown to be missense mutations. All these mutations affected the coiled-coil domain, which plays a key role in unphosphorylated STAT1 dimerization and STAT1 nuclear dephosphorylation (Fig. 1, A and C; Chen et al., 1998; Levy and Darnell, 2002; Braunstein et al., 2003; Zhong et al., 2005; Hoshino et al., 2006; Mertens et al., 2006). We therefore sequenced the corresponding coding region of *STAT1* (exons 6 to 10) in another 106 patients, including 57 with sporadic CMCD and 49 from 22 multiplex kindreds with AD CMCD. 29 patients from 16 kindreds were heterozygous for a *STAT1* missense mutation (Fig. 1, A and B, Kindreds C-F, H-K, and M-T; Fig. 1 C; and Table I; Table S3). In total, 36 patients from 20 kindreds were heterozygous for 1 of the 12 missense mutations identified that affected the coiled-coil domain of STAT1. 11 other CMCD patients in these kindreds were not genotyped. The intrafamilial segregation of the mutations was consistent with an AD trait, as all patients with CMCD from the kindreds tested were heterozygous, whereas none of these mutations was found in the heterozygous state in any of the healthy relatives tested (Fig. 1 B). Moreover, the *STAT1* haplotypes for common SNPs indicated that the five recurrent mutations were caused by mutation hotspots rather than founder effects (unpublished data). Finally, the mutations were found to have occurred de novo in at least four kindreds, which is consistent with a high clinical penetrance of these alleles. The mutations were not found in the National Center for Biotechnology Information, Ensembl, and dbSNP databases. They were also absent from 1,052 controls from 52 ethnic groups in the Centre d'Etude du Polymorphisme Humain and Human Genome Diversity panels, suggesting that they were rare, CMCD-inducing variants rather than irrelevant polymorphisms.

The 12 missense mutations were not conservative and were therefore predicted to affect protein structure and function. Moreover, most of the affected residues were found to have been conserved throughout evolution in the species in which *STAT1* had been sequenced (Table S3). Accordingly, POLYphen II predicted that all but one of these mutations would be possibly or probably damaging (Adzhubei et al., 2010; Table S3). None of the previously described nine patients with AD STAT1 deficiency and MSMD was heterozygous for mutations affecting the coiled-coil domain (Fig. 1, A and C; Dupuis et al., 2001; Chapgier et al., 2006a; Averbuch et al., 2011; unpublished data). However, three of the eight patients with AR STAT1 deficiency and susceptibility to intracellular bacterial and viral diseases, who, like their heterozygous relatives, did not display CMC, carried mutations affecting the coiled-coil domain (Fig. 1, A and C; Chapgier et al., 2009; Chapgier et al., 2006b; Dupuis et al., 2003; Kong et al., 2010; Kristensen et al., 2011; Averbuch et al., 2011). These three patients from two kindreds carried the K201N or K211R mutation (Kong et al., 2010; Kristensen et al., 2011). Nevertheless, the three-dimensional structure of phosphorylated STAT1 molecules revealed that the 12 CMCD-linked missense mutations affected a cluster of residues located in a specific pocket of the coiled-coil domain, near residues essential for STAT1 dephosphorylation (Fig. 1 C; Chen et al., 1998; Zhong et al., 2005; Mertens et al., 2006). In contrast, the other two morbid mutations (K201N and K211R) affect residues located on the other side of the coiled-coil domain (Fig. 1 C). Moreover, these two hypomorphic alleles were shown to be pathogenic not because they were missense, but because they promoted the splicing out of exon 8, resulting in AR partial STAT1 deficiency, with the production of small amounts of intrinsically functional STAT1 molecules (Kong et al., 2010; Kristensen et al., 2011). These genetic data strongly suggest that heterozygous missense mutations in the coiled-coil domain of STAT1 may cause AD CMCD in a large fraction of patients. Nevertheless, the occurrence of other germline mutations in *STAT1* in patients without CMC and with an AD or AR predisposition to other infectious diseases raised questions about whether these mutations were really responsible for CMCD and the underlying mechanism of disease.

We functionally characterized the CMCD-causing *STAT1* allele R274Q, which was found in four kindreds (Fig. 1 B and Table I). We compared it with a WT and an MSMD-causing loss-of-function *STAT1* allele (L706S; Dupuis et al., 2001). We transfected STAT1-deficient U3C fibrosarcoma cells with WT, R274Q, or L706S *STAT1* alleles. Upon stimulation with IFN-α, IFN-γ, or IL-27, cells transfected with the R274Q allele responded two to three times more strongly than those transfected with the WT allele, as shown by measurement of the induction of γ-activated sequence (GAS)–dependent reporter gene transcription activity, with mock- and L706S-transfected cells serving as negative controls (Fig. 2 A and Fig. S1 A). All *STAT1* alleles were expressed at an equal strength, as shown by Western blotting (WB; Fig. 2 B). Higher levels of STAT1 phosphorylation were observed for the R274Q allele than for the WT allele after stimulation with IFN-γ, IFN-α, and IL-27, whereas STAT3 phosphorylation levels were similar for the two alleles (Fig. 2 B). In contrast, the induction of IFN-stimulated response element (ISRE)–dependent transcription activity by IFN-α was normal (Fig. S1, B and C). In the same experimental conditions, the other 10 CMCD-associated *STAT1* alleles tested were also gain-of-function, unlike the K201N and K211R alleles (Fig. S1 D). Upon stimulation with IFN-γ, IFN-α, or IL-27, an increase in GAS-binding activity was detected in cells transfected with the R274Q allele (Fig. S1 E). Accordingly, the transcription of the *CXCL9* and *CXCL10* target genes was enhanced (Fig. 2, C and D). Overall, these data indicate that at least 11 of the 12 CMCD-linked *STAT1* missense alleles are intrinsically gain-of-function.

The mechanism involved an increase in STAT1 tyrosine 701 residue phosphorylation, as shown for R274Q by WB after stimulation with IFN-α, IFN-γ, and IL-27 (Fig. 2 B). STAT1 was not constitutively activated, and STAT3 was normally activated in R274Q-transfected cells (Fig. 2 B and not depicted). Almost all the mutant STAT1 molecules, which were phosphorylated in response to IFN-γ, translocated to and accumulated in the nucleus, as shown by immunofluorescence (Fig. S1 F). WB showed R274Q STAT1 to be more

Published July 4, 2011

JEM

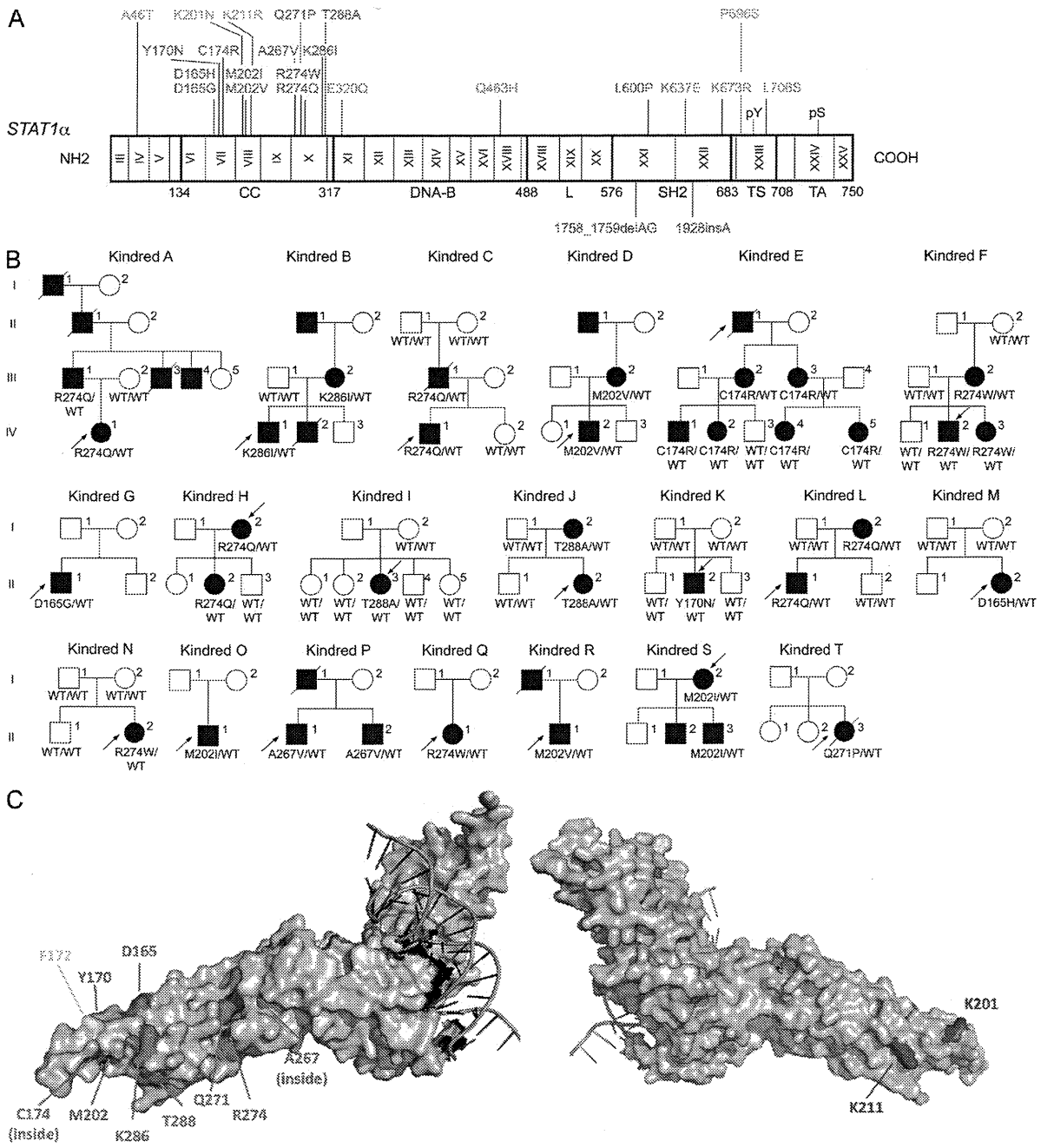

Figure 1. Heterozygous missense mutations affecting the STAT1 coiled-coil domain in kindreds with AD CMCD. (A) The human *STAT1* α isoform is shown, with its known pathogenic mutations. Coding exons are numbered with roman numerals and delimited by a vertical bar. Regions corresponding to the coiled-coil domain (CC), DNA-binding domain (DNA-B), linker domain (L), SH2 domain (SH2), tail segment domain (TS), and transactivator domain (TA) are indicated, together with their amino-acid boundaries, and are delimited by bold lines. Tyr701 (pY) and Ser727 (pS) are indicated. Mutations in green are dominant and associated with partial STAT1 deficiency and MSMD. Mutations in brown are recessive and associated with complete STAT1 deficiency and intracellular bacterial and viral disease. Mutations in blue are recessive and associated with partial STAT1 deficiency and intracellular bacterial and/or viral disease. Mutations in red are dominant and associated with a gain-of-function of STAT1 and CMCD. (B) Pedigrees of 20 families with AD "gain-of-function" *STAT1* mutations. Each kindred is designated by a letter (A to T), each generation is designated by a roman numeral (I-II-III-IV), and each individual is designated by an Arabic numeral (each individual studied is identified by a code of this type, organized from left to right). Black indicates CMCD patients. The probands are indicated by arrows. When tested, the genotype for *STAT1* is indicated below each individual. (C) Three-dimensional structure of phosphorylated STAT1 in complex with DNA. Connolly surface representation, with the following amino acids highlighted: red, amino acids mutated in patients with CMCD; blue, amino acids located in the coiled-coil domain and mutated in patients with MSMD and viral diseases; yellow, amino acids identified in vitro as affecting the dephosphorylation process.

Published July 4, 2011

Table I. Summary of the clinical and genetic data for the patients

Patient	Age at presentation	Origin	Clinical features of CMC	Cause of death (age/yr)	Autoimmunity	Genotype
A-I-1	-	France	Nails	Not related to the disease (old age)	None	-
A-II-1	-	France	Nails	Not related to the disease (old age)	None	-
A-III-1	1 mo	France	Nails, oral cavity, oropharynx, genital mucosa		None	WT/R274Q
A-III-3	-	France	Nails, oral cavity	Not related to the disease (40)	None	-
A-III-4	-	France	Nails, oral cavity		None	-
A-IV-1	1 mo	France	Nails, oral cavity, oropharynx		None	WT/R274Q
B-II-1	-	France	-		None	-
B-III-2	3 yr	France	Skin, nails, oral cavity, oropharynx, genital mucosa		None	WT/K286I
B-IV-1	5 yr	France & Congo	Skin, nails, oral cavity, oropharynx		None	WT/K286I
B-IV-2	5 mo	France & Congo	Skin, nails, oral cavity, oropharynx	Cerebral aneurysm (8)	None	-
C-III-1	-	Turkey	Nails, oral cavity, genital mucosa	Cerebral aneurysm (34)	Thyroid autoimmunity	WT/R274Q
C-IV-1	-	Turkey	Nails, oral cavity		None	WT/R274Q
D-II-1	-	France	Nails, oral cavity, genital mucosa		-	-
D-III-2	7 yr	France	Skin, oral cavity, oropharynx		None	WT/M202V
D-IV-2	1 mo	France	Skin, nails, oropharynx		Thyroid autoimmunity	WT/M202V
E-II-1	1 yr	Germany	Skin, oral cavity, oropharynx	Squamous cell carcinoma (54)	-	-
E-III-2	1 yr	Germany	Nails, oral cavity, oropharynx, genital mucosa		Thyroid autoimmunity	WT/C174R
E-III-3	9 mo	Germany	Skin, nails, oral cavity, oropharynx, genital mucosa		Thyroid autoimmunity	WT/C174R
E-IV-1	18 mo	Germany	Skin, oral cavity, oropharynx, genital mucosa		None	WT/C174R
E-IV-2	2 yr	Germany	Skin, oral cavity, oropharynx		Thyroid autoimmunity	WT/C174R
E-IV-4	2 yr	Germany	Skin, oral cavity, oropharynx, genital mucosa		None	WT/C174R
E-IV-5	1 yr	Germany	Skin, nails, oral cavity, oropharynx		None	WT/C174R
F-III-2	1 mo	Argentina	Nails, oral cavity, oropharynx, genital mucosa		-	WT/R274W
F-IV-2	1 mo	Argentina	Skin, nails, oral cavity, oropharynx		-	WT/R274W
F-IV-3	6 mo	Argentina	Nails, oral cavity, genital mucosa		-	WT/R274W
G-II-1	3 mo	Ukrainian	Nails, skin, oral cavity, oropharynx, esophagus		None	WT/D165G
H-I-2	1 yr	Japan	Skin, oropharynx, esophagus		-	WT/R274Q
H-II-2	5 yr	Japan	Oral cavity, oropharynx		-	WT/R274Q
I-II-3	9 mo	Mexico	Skin, nails, oral cavity, genital mucosa		None	WT/T288A
J-I-2	-	Switzerland	Oral cavity, oropharynx		None	WT/T288A
J-II-2	3 mo	Switzerland	Oral cavity, oropharynx		-	WT/T288A
K-II-2	11 mo	Switzerland	Nails, oral cavity, oropharynx		Thyroid autoimmunity	WT/Y170N
L-I-2	7 yr	France	Skin, nails, oropharynx, esophagus		Thyroid autoimmunity	WT/R274Q
L-II-1	1 mo	France	Skin, nails, oropharynx, esophagus		None	WT/R274Q
M-II-2	6 mo	Germany	Skin, nails, oropharynx, genital mucosa		Thyroid autoimmunity	WT/D165H

Published July 4, 2011

JEM

Table I. Summary of the clinical and genetic data for the patients *(Continued)*

Patient	Age at presentation	Origin	Clinical features of CMC	Cause of death (age/yr)	Autoimmunity	Genotype
N-II-2	1 yr	Germany	Skin, nails, oropharynx	Squamous cell carcinoma (54)	None	WT/R274W
O-II-1	18 mo	Germany	Oral cavity, oropharynx		None	WT/M202I
P-I-1	1 yr	Israel	Oropharynx, genital mucosa	Not related to the disease (46)	None	-
P-II-1	<2 yr	Israel	Skin, nails, oropharynx		None	WT/A267V
P-II-2	<2 yr	Israel	Skin, nails, oropharynx		None	WT/A267V
Q-II-1	1 mo	France	Skin, oral cavity, oropharynx, genital mucosa		None	WT/R274W
R-I-1	4 yr	France	Skin, nails, oropharynx	Squamous cell carcinoma (55)	None	-
R-II-1	18 mo	France	Lips, oropharynx		None	WT/M202V
S-I-2	6 mo	France	Skin, oral cavity, oropharynx		Systemic lupus erythematosus	WT/M202I
S-II-2	1 yr	France	Nails		None	-
S-II-3	1 mo	France	Skin, oropharynx		None	WT/M202I
T-II-3	1 yr	Germany	Skin, nails, oropharynx	Squamous cell carcinoma (41)	None	WT/Q271P

None of the patients displays autoantibodies against IL-17A, IL-17F, and IL-22. -, unknown.

strongly phosphorylated than the WT protein in both cytoplasmic and nuclear extracts (Fig. S1 G). The mechanism underlying the gain of R274Q phosphorylation was explored with the tyrosine kinase inhibitor staurosporine and the phosphatase inhibitor pervanadate. The dephosphorylation of IFN-γ–activated R274Q STAT1 was impaired by staurosporine, but less than that of the known dephosphorylation mutant F77A (Fig. 2 E; Zhong et al., 2005). In contrast, pervanadate normalized the phosphorylation of R274Q to WT levels (Fig. 2 F). Another CMCD-linked mutation, D165G (Fig. 1, A–C), also resulted in impaired dephosphorylation that could be normalized by adding pervanadate (Fig. 2 F and Fig. S1 H). Thus, at least two CMCD-linked *STAT1* missense alleles (R274Q and D165G) are gain-of-function caused by the impairment of nuclear dephosphorylation. These alleles may therefore enhance cellular responses to cytokines activating STAT1 predominantly and STAT3 to a lesser extent, such as IFN-α/β, IFN-γ, IFN-λ, and IL-27, and possibly also responses to cytokines activating STAT3 predominantly and STAT1 to a lesser extent, such as IL-6, IL-21, IL-22, and IL-23 (Fig. S2).

We investigated the dominance of the *STAT1* alleles at the cellular level by testing EBV-B–transformed (EBV-B) cells and SV-40–transformed dermal fibroblasts from a CMCD patient heterozygous for the *STAT1* R274Q allele. We observed enhanced IFN-α/β–, IFN-γ–, and IL-27–dependent STAT1 phosphorylation in EBV-B cells from a patient heterozygous for the *STAT1* R274Q allele, as shown by WB (Fig. 3, B and D). Phospho-STAT1 accumulated in the nucleus of R274Q heterozygous SV-40 fibroblasts upon IFN-γ stimulation, as well as in EBV-B cells (Fig. 3 I and Fig. S3 D). Moreover, the IFN-α/β–, IFN-γ–, and IL-27–induced DNA-binding activity of GAF was stronger in cells from the CMCD patient than in those from a healthy control or from a MSMD patient carrying the L706S mutant allele, as shown by electrophoretic mobility shift assay (EMSA; Fig. 3, A and C). In contrast, the DNA-binding activity of ISGF-3 seemed to be normal in cells from the patient stimulated with IFN-α/β (Fig. S3 A). These data strongly suggest that the heterozygous R274Q allele is dominant for STAT1-dependent responses and gain-of-function for GAF-dependent cellular responses to key STAT1-activating cytokines, such as IFN-α/β, IFN-γ, and IL-27. The mutation may also affect IFN-λ responses.

We then tested cytokines that predominantly activate STAT3, rather than STAT1, such as IL-6, IL-21, IL-22, and IL-23 (Hunter, 2005; Kishimoto, 2005; Kastelein et al., 2007; Spolski and Leonard, 2008; Donnelly et al., 2010; Sabat, 2010; Ouyang et al., 2011). Peripheral T cell blasts from a patient displayed normal STAT3 activation in response to IL-23, as shown by WB (Fig. S3 B). No increase in STAT1 phosphorylation was detected in cells from a patient or controls upon IL-23 stimulation. Furthermore, fibroblasts from a patient displayed normal activation of STAT3 in response to IL-22 (Fig. S3 C). In the same conditions, no STAT1 phosphorylation was detected in cells from the patient or controls (unpublished data). In contrast, the levels of STAT1 phosphorylation in response to IL-6 and IL-21 were higher in the patient's EBV-B cells than in cells from healthy controls and from a patient with MSMD heterozygous for the L706S allele, whereas STAT3 activation was normal as shown by WB (Fig. 3, F and H). Consistent with these findings, stronger GAS activity was observed in cells from the patient in response to IL-6 and IL-21 stimulation (Fig. 3, E and G). These data suggest that heterozygous missense mutations in the coiled-coil domain of STAT1 are dominant and gain-of-function for GAF-dependent cellular responses for cytokines that predominantly activate STAT3, such as IL-6 and IL-21. Overall, these data suggest that the *STAT1* alleles are truly responsible for CMCD in these kindreds and raise questions about the immunological basis of CMCD.

Published July 4, 2011

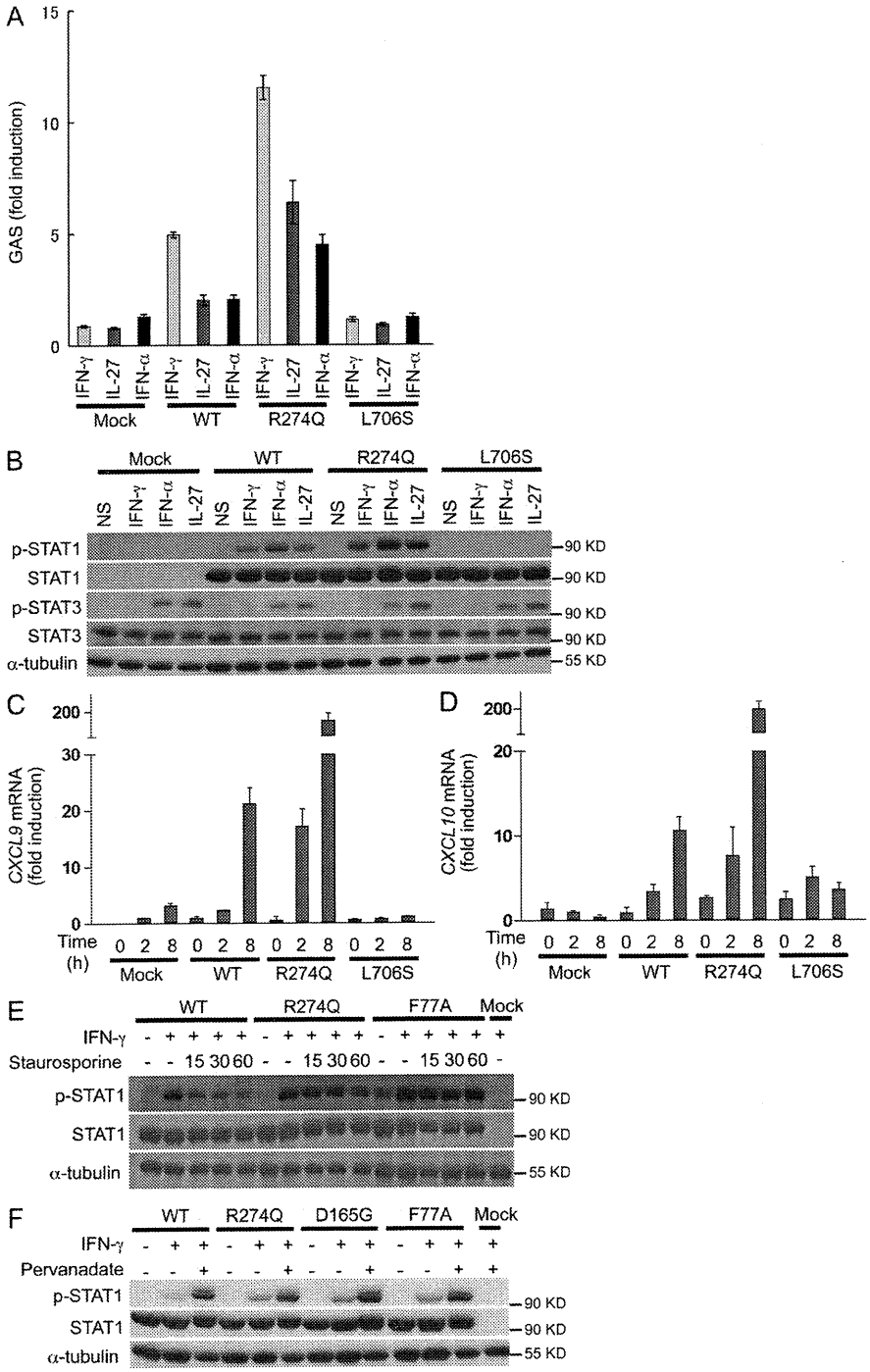

Figure 2. The mutant R274Q *STAT1* allele is gain-of-phosphorylation and gain-of-function for GAF-dependent cellular responses. U3C cells were transfected with a mock vector, a WT, or two mutant alleles of *STAT1* (R274Q and L706S). The response to IFN-γ, IL-27, and IFN-α was then evaluated by determining luciferase activity of a reporter gene under the control of the GAS promoter (A), and by determining STAT1 and STAT3 phosphorylation by Western blot (B). Experiments were performed at least three times independently. (C and D) Quantitative RT-PCR was used to measure the induction of *CXCL9* (C) and *CXCL10* (D) 2–8 h after stimulation with IFN-γ. Experiments were performed two times independently. (E) The nuclear dephosphorylation of STAT1 was tested by WB in U3C cells transfected with a mock vector, WT *STAT1*, the R274Q, or the F77A (a known loss-of-dephosphorylation mutant) *STAT1* mutant alleles, and treated with IFN-γ with or without the tyrosine kinase inhibitor staurosporine for the indicated periods of time (in minutes). Three independent experiments were performed. (F) Western blot of U3C cells transfected with mock, WT, R274Q, D165G, and F77A alleles of *STAT1*, nontreated or treated with IFN-γ in the absence or presence of the phosphatase inhibitor pervanadate. Two independent experiments were performed. Error bars represent SD of one experiment done in triplicate (Fig. S1 D).

IL-27 is a potent inhibitor of the development of IL-17–producing T cells in mice (Batten et al., 2006; Stumhofer et al., 2006; Yoshimura et al., 2006; Amadi-Obi et al., 2007; Diveu et al., 2009; El-behi et al., 2009; Villarino et al., 2010) and humans (Diveu et al., 2009; Liu and Rohowsky-Kochan, 2011), through a mechanism dependent on STAT1 (Amadi-Obi et al., 2007; Batten et al., 2006; Diveu et al., 2009; Liu and Rohowsky-Kochan, 2011; Stumhofer et al., 2006; Villarino et al., 2010). Moreover, mouse IFN-γ (Feng et al., 2008; Tanaka et al., 2008; Villarino et al., 2010) and human IFN-α/β (Chen et al., 2009; Ramgolam et al., 2009) have been shown to antagonize the development of IL-17–producing T cells via STAT1. In addition, IL-6, IL-21, and IL-23 are prominent inducers of IL-17–producing T cells, via a mechanism dependent on STAT3 and antagonized by STAT1 (Hirahara et al., 2010). Finally, we recently showed that inborn errors of IL-17F or IL-17RA were genetic etiologies of CMCD (Puel et al., 2010b, 2011). We thus determined the proportion of IL-17A– and IL-22–producing T cells by flow cytometry in patients with heterozygous *STAT1* mutations and AD CMCD. The 18 CMCD patients carrying gain-of-function mutations in *STAT1* that were tested had lower proportions of circulating IL-17A– and IL-22–producing T cells ex vivo than 28 healthy controls ($P < 10^{-4}$) and six patients bearing loss-of-function *STAT1* alleles ($P < 2.10^{-3}$; Fig. 4, A and B; and Fig. S4 G). In contrast, they displayed normal proportions of IFN-γ–producing T cells (Fig. S4 F).

Published July 4, 2011

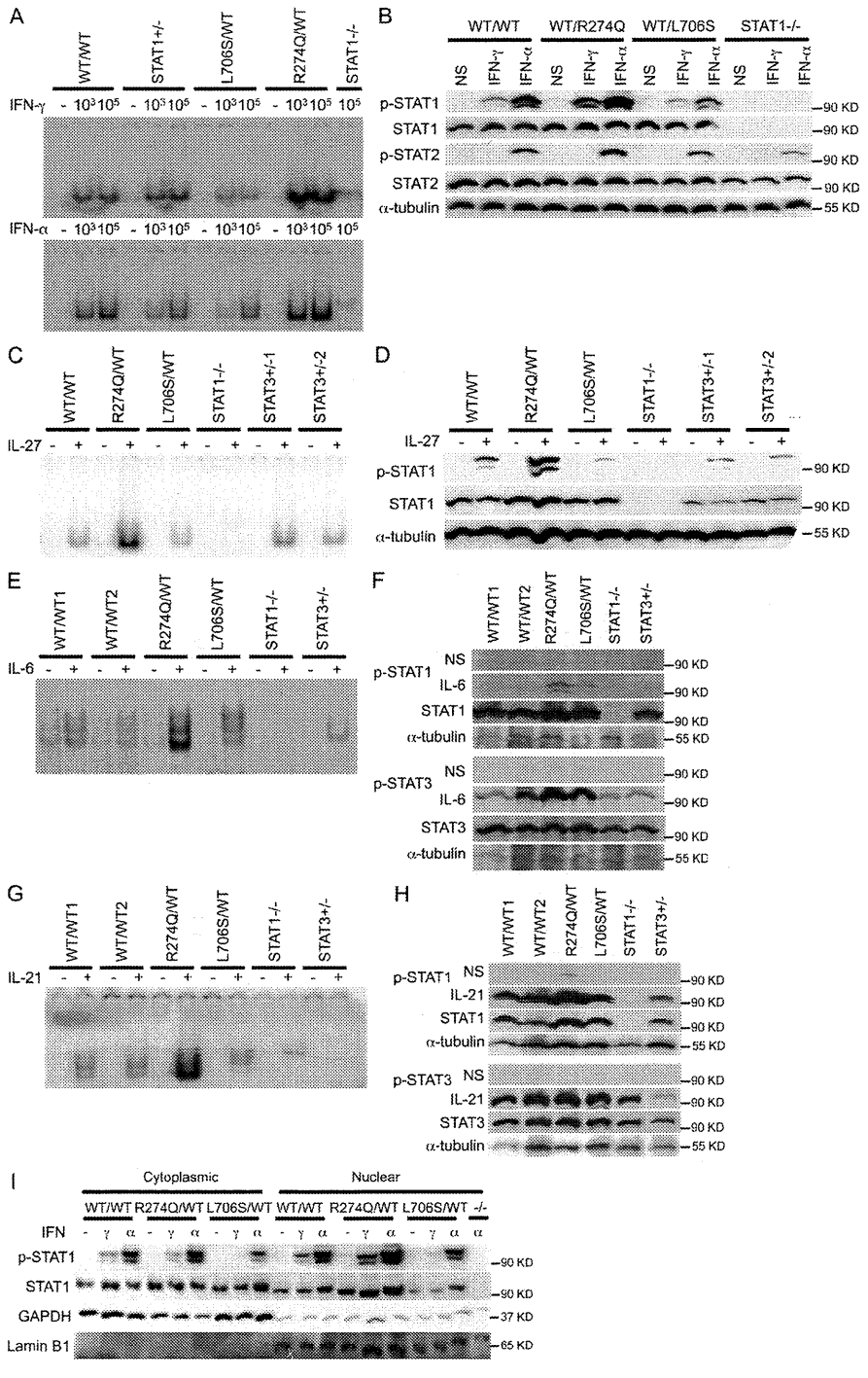

Figure 3. The mutant R274Q *STAT1* allele is dominant for GAF-dependent cellular responses at the cellular level. The responses of the patient's EBV-B cells (R274Q/WT) were evaluated independently at least twice, by EMSA, with a GAS probe (A, C, E, and G), and by Western blot (B, D, F, and H). This response was compared with that of one or two healthy controls (WT/WT1 and WT/WT2), heterozygous cells with a WT and a loss-of-function *STAT1* allele (STAT1$^{+/-}$), cells heterozygous for a dominant loss-of-function mutation of *STAT1* (L706S/WT), cells with complete STAT1 deficiency (STAT1$^{-/-}$), and cells from two patients heterozygous for dominant loss-of-function mutations of *STAT3* (STAT3$^{+/-1}$ and STAT3$^{+/-2}$). Cells were left nonstimulated (NS) or stimulated, as indicated, with IFN-γ, IFN-α, IL-27, IL-6, and IL-21. pSTAT is an antibody specific for STAT with a phosphorylated tyrosine residue. (I) The nuclear and cytoplasmic fractions of EBV-B cells from a control (WT/WT), a CMCD patient (R274Q/WT), a heterozygous patient with a dominant loss-of-function mutation of *STAT1* (L706S/WT) and a patient with complete STAT1 deficiency ($^{-/-}$) stimulated with IFN-γ and IFN-α were tested for the presence of phosphorylated STAT1 and STAT1 by WB. Antibodies directed against GAPDH and Lamin B1 were used to normalize the amount of cytoplasmic and nuclear proteins, respectively. The experiment was performed twice.

Moreover, only very small amounts of IL-17A, IL-17F, and IL-22 were secreted by freshly prepared leukocytes after ex vivo stimulation with PMA and ionomycin ($P < 8.10^{-3}$), as shown by ELISA (Fig. 4, C–E). In contrast, the amounts of secreted IL-17A, IL-17F, and IL-22 were normal in patients heterozygous or homozygous for loss-of-function or hypomorphic *STAT1* mutations (Fig. 4, C–E). Interestingly, in all assays, the proportions of IL-17A– and IL-22–producing T cells and the amounts of IL-17A, IL-17F, and IL-22 secreted were smallest for the four patients with the most apparently severe clinical phenotype (Fig. 4, A–E and not depicted).

After the culture of PBMCs in vitro in the presence of various cytokines, including IL-6, TGF-β, IL-1β, and IL-23, the proportion of IL-17A– and IL-22–producing T cell blasts remained significantly lower ($P < 10^{-4}$) in CMCD patients carrying *STAT1* mutations than in controls (Fig. S4, A and B; and not depicted). In contrast, the proportions of IL-17A– and IL-22–producing T cell blasts were normal in patients with loss-of-function *STAT1* mutations (Fig. S4, A and B; and not depicted). The amounts of IL-17A, IL-17F, and IL-22 in the supernatant of T cell blasts stimulated with PMA and ionomycin after culture in vitro were also significantly lower in patients with *STAT1* mutations and CMCD ($P < 4.10^{-4}$; Fig. S4, C–E; and not depicted). In contrast, patients with loss-of-function mutant *STAT1* alleles displayed normal levels of cytokine secretion (Fig. S4, C–E; and not depicted). Finally, levels of IL-12p70 and

Published July 4, 2011

IL-12p40 production by whole blood stimulated with IFN-γ were higher in CMCD patients bearing gain-of-function *STAT1* alleles than in patients bearing loss-of-function *STAT1* alleles and healthy controls (Fig. 4 F and not depicted). Thus, patients with familial or sporadic AD CMCD heterozygous for mutations affecting the coiled-coil domain of STAT1, including the dominant gain-of-function R274Q mutant allele, displayed lower levels of IL-17 cytokine production by peripheral T cells, providing a molecular mechanism for the disease.

DISCUSSION

We have shown that several germline missense mutations affecting the coiled-coil domain of STAT1 may cause sporadic and familial AD CMCD. The underlying mechanism involves a gain of STAT1 phosphorylation caused by the loss of nuclear dephosphorylation, resulting in a gain-of-function of GAF in response to various cytokines. Impaired dephosphorylation may not be the only mechanism influencing the impact of these mutations on the transcription of STAT1 target genes, as these mutations may also affect other processes, such as the dimerization of unphosphorylated STAT1. Moreover, the gain-of-function, which manifests itself in terms of DNA-binding activity, reporter gene induction, and target gene induction, may not necessarily increase the transcription of all target genes, possibly even resulting in the repression of some genes. In addition, the various *STAT1* mutations, although they all affect the coiled-coil domain and are probably all loss-of-dephosphorylation and gain-of-function, may somewhat differ from each other in terms of their functional impact. The genome-wide impact of these mutations on the transcriptome remains to be assessed in various cell types stimulated with a range of cytokines. In any case, the gain-of-function mutant *STAT1* alleles were dominant for GAF activation in all cell types tested. They affected cellular responses to various cytokines, including IFN-α/β, IFN-γ, and IL-27, which predominantly activate STAT1 over STAT3, and IL-6 and IL-21, which predominantly activate STAT3 over STAT1. These mutations probably also strengthen cellular responses to IFN-λ. However, they do not seem to affect STAT1-containing ISGF-3 activation by IFN-α/β, at least in the conditions tested. Moreover, STAT3 activation by IL-6, IL-21, IL-22, and IL-23 is maintained, suggesting that STAT3 activation by IL-26 is also intact.

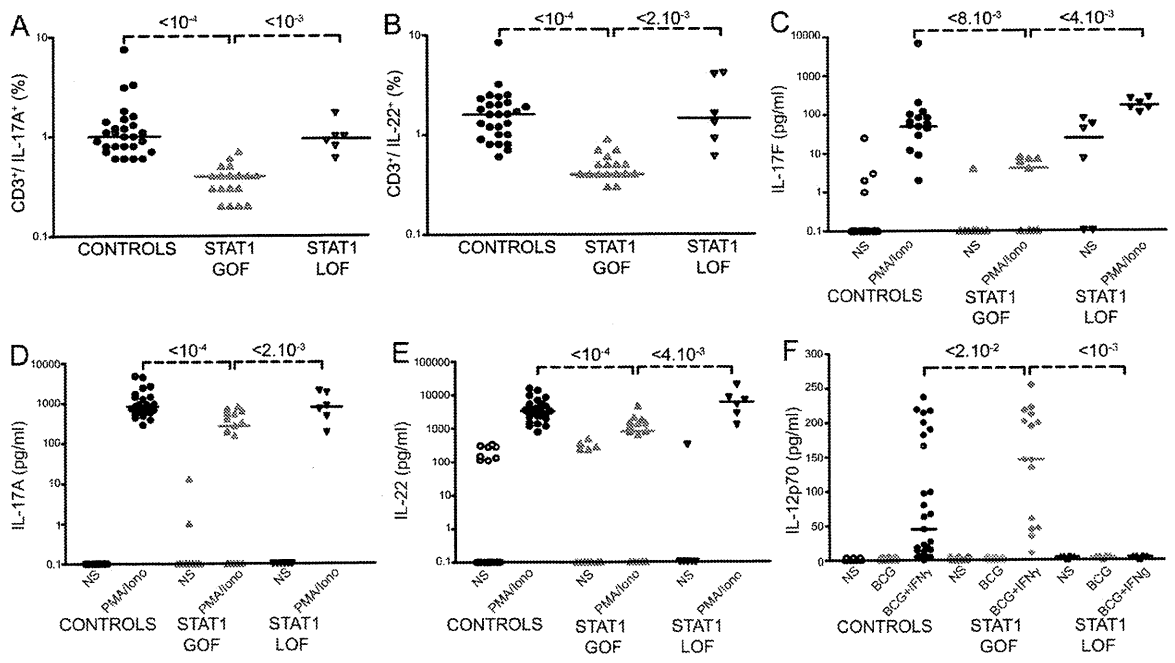

Figure 4. Impaired development and function of IL-17– and IL-22–producing T cells ex vivo in patients with AD CMCD and *STAT1* mutations. Each symbol represents a value from a healthy control individual (black circles), a patient bearing a *STAT1* gain-of-function (GOF) allele (red upright triangles), or a patient bearing one or two *STAT1* loss-of-function (LOF) alleles (black upside-down triangles). (A and B) Percentage of $CD3^+/IL\text{-}17A^+$ (A) and $CD3^+/IL\text{-}22^+$ (B) cells, as determined by flow cytometry, in nonadherent PBMCs activated by incubation for 12 h with PMA and ionomycin. (C–E) Secretion of IL-17F (C), IL-17A (D) and IL-22 (E) by whole blood cells, as determined by ELISA, in the absence of stimulation (open symbols) and after stimulation with PMA and ionomycin for 48 h (closed symbols). Horizontal bars represent medians. The p-values for the nonparametric Wilcoxon test, between patients with *STAT1* GOF mutations ($n = 18$) and controls ($n = 28$) and patients with *STAT1* LOF mutations ($n = 6$) are indicated. All differences between healthy controls and patients with *STAT1* LOF alleles were not significant. (F) Secretion of IL-12p70 by whole blood cells, as determined by ELISA, in the absence of stimulation (open symbols), after stimulation with BCG (lightly colored symbols), or BCG + IFN-γ for 48 h (closed symbols). Horizontal bars represent medians. The p-values for differences between patients with *STAT1* GOF mutations ($n = 15$) and controls ($n = 23$) and patients with *STAT1* LOF mutations ($n = 6$) are indicated and were calculated in nonparametric Wilcoxon tests. All experiments were performed at least two times independently.

Published July 4, 2011

The mutant *STAT1* alleles described herein enhance cellular responses to cytokines such as IFN-α/β, IFN-γ, and IL-27, which potently inhibit the development of IL-17–producing T cells via STAT1 (Batten et al., 2006; Yoshimura et al., 2006; Stumhofer et al., 2006; Amadi-Obi et al., 2007; Feng et al., 2008; Kimura et al., 2008; Tanaka et al., 2008; Chen et al., 2009; Ramgolam et al., 2009; Crabé et al., 2009; Diveu et al., 2009; El-behi et al., 2009; Guzzo et al., 2010; Villarino et al., 2010; Liu and Rohowsky-Kochan, 2011). These mutant alleles also increase cellular responses to IL-6 and IL-21, which normally induce IL-17–producing T cells via STAT3 rather than STAT1 (Hirahara et al., 2010). Enhanced STAT1-dependent cellular responses to these two groups of cytokines probably impair the development of IL-17–producing T cells. It remains unclear whether this mechanism predominantly involves IL-17–inhibiting cytokines (IFN-α/β, IFN-γ, and IL-27), either individually or in combination. The available data from the mouse model suggest that IL-27 is the most potent of the three inhibitors. There is also evidence that these cytokines inhibit IL-17–producing T cell development in humans (Ramgolam et al., 2009; Liu and Rohowsky-Kochan, 2011). Enhanced STAT1 and GAF activation in response to the IL-17 inducers IL-6 and IL-21, and perhaps IL-23, may also play a key role in disease, by antagonizing STAT3 responses. The effect of the aryl hydrocarbon receptor on IL-17 T cell development might also be enhanced by gain-of-function *STAT1* alleles (Kimura et al., 2008). Moreover, enhanced STAT1 activity downstream from IL-22 and IL-26 in cells, not detected in our study, might also contribute to the CMCD phenotype. Finally, thyroid autoimmunity in eight patients and systemic lupus erythematosus in another patient in our series probably resulted from the enhancement of IFN-α/β responses, as such autoimmunity is a frequent adverse effect of treatment with recombinant IFN-α or IFN-β (Oppenheim et al., 2004; Selmi et al., 2006). Importantly, no autoantibodies against IL-17A, IL-17F, or IL-22 were detected in the patients' serum (Table I and unpublished data).

Remarkably, germline mutations in human *STAT1* underlie susceptibility to three different types of infectious disease: mycobacterial diseases, viral diseases, and CMC. Patients bearing *STAT1* mutations and displaying mycobacterial and/or viral disease do not suffer from CMC, and the patients with CMCD caused by other *STAT1* alleles described here present no mycobacterial or viral disease. The pathogenic mechanisms involved are clearly different, with loss-of-function mutations in *STAT1* underlying mycobacterial and viral diseases (Dupuis et al., 2001, 2003; Chapgier et al., 2006b, 2009; Kong et al., 2010; Averbuch et al., 2011; Kristensen et al., 2011). Human AR STAT1 deficiency impairs cellular responses to IFN-α/β, IFN-γ, IFN-λ, and IL-27 (Dupuis et al., 2003; Chapgier et al., 2006b, 2009; Kong et al., 2010; Kristensen et al., 2011). Viral diseases probably result from impaired IFN-α/β and, perhaps, IFN-λ immunity, although impaired IFN-γ and IL-27 immunity may also contribute to the phenotype. Patients with AD MSMD, heterozygous for loss-of-function dominant-negative mutations of *STAT1*, suffer from mycobacterial disease caused by the impairment of IFN-γ immunity (Chapgier et al., 2006a; Dupuis et al., 2001). Overall, mutations impairing STAT1 function confer AD or AR susceptibility to intracellular agents, through the impairment of IFN-α/β (viral diseases) and/or IFN-γ immunity (mycobacterial diseases). In contrast, the gain-of-function *STAT1* mutations reported here confer AD CMCD because of the enhancement of STAT1-mediated cellular responses to STAT1-dependent repressors and STAT3-dependent inducers of IL-17–producing T cells. These studies neatly demonstrate that severe infectious diseases in otherwise healthy patients may be subject to genetic determinism (Casanova and Abel, 2005, 2007; Alcaïs et al., 2009, 2010). They also highlight the profoundly different effects that germline mutations in the same human gene may have, resulting in different infectious diseases through different molecular and cellular mechanisms.

MATERIALS AND METHODS

Massively parallel sequencing

DNA (3 µg) extracted from EBV-B cells from the patient was sheared with a S2 Ultrasonicator (Covaris). An adapter-ligated library was prepared with the Paired-End Genomic DNA Sample Prep kit (Illumina). The SureSelect Human All Exon kit (Agilent Technologies) was then used for exome capture. Single-end sequencing was performed on a Genome Analyzer IIx (Illumina), generating 72-base reads.

Sequence alignment, variant calling, and annotation

BWA aligner (Li and Durbin, 2009) was used to align the sequences obtained with the human genome reference sequence (hg18 build). Downstream processing was performed with the Genome analysis toolkit (GATK; McKenna et al., 2010), SAMtools (Li et al., 2009), and Picard Tools (http://picard.sourceforge.net). Substitution calls were made with a GATK UnifiedGenotyper, whereas indel calls were made with a GATK IndelGenotyperV2. All calls with a read coverage ≤2x and a Phred-scaled SNP quality of ≤20 were filtered out. All the variants were annotated with annotation software that was developed in-house. The data were further analyzed with sequence analysis software that had been developed in-house (SQL database query–driven system).

Molecular genetics

EBV-B cells and the STAT1-deficient cell line U3C were cultured as previously described (Chapgier et al., 2006a). Primary fibroblasts were cultured in DME supplemented with 10% fetal calf serum. Cells were stimulated with the indicated doses (in IU/ml or ng/ml) of IFN-γ (Imukin; Boehringer Ingelheim), IFN-α2b (IntronA; Schering-Plough), IL-27 (R&D Systems), IL-21 (R&D Systems), IL-22 (R&D Systems), IL-23 (R&D Systems), and IL-6 (R&D Systems). Genomic DNA and total RNA were extracted from cell lines and fresh blood cells, as previously described (Chapgier et al., 2006a). Genomic DNA was amplified with specific primers encompassing exons 6–10 of *STAT1* (available upon request), sequenced with the Big Dye Terminator cycle sequencing kit (Applied Biosystems), and analyzed on an ABI Prism 3730 (Applied Biosystems). We used the various alleles of *STAT1* in the pcDNA3 *STAT1*-V5 vector (Chapgier et al., 2006a; Kong et al., 2010). We generated the various *STAT1* mutations by site-directed mutagenesis (QuikChange Site-Directed Mutagenesis kit; Stratagene) with the mismatched primers listed in Table S4. U3C cells were harvested by trypsin treatment 24 h before transfection and replated at a density of 2.5×10^5 cells/ml in 6-well plates. Plasmid DNA (5 µg per plate) carrying the WT or all the various mutant *STAT1* alleles was used for cell transfection with the Calcium Phosphate Transfection kit (Invitrogen).

Luciferase reporter assay

U3C cells were dispensed into 96-well plates (1×10^4/well) and transfected with reporter plasmids (Cignal GAS and ISRE Reporter Assay kit;

Published July 4, 2011

SABiosciences) and plasmids carrying the various alleles of *STAT1* or a mock vector, in the presence of Lipofectamine LTX (Invitrogen). 6 h after transfection, the cells were transferred back into medium containing 10% FBS and cultured for 24 h. The transfectants were then stimulated with IFN-γ (500 and 1,000 IU/ml), IL-27 (20 and 100 ng/ml), and IFN-α (500, 1,000, and 5,000 IU/ml) for 16 h and subjected to luciferase assays with the Dual-Glo luciferase assay system (Promega). Experiments were performed in triplicate and firefly luciferase activity was normalized with respect to *Renilla* luciferase activity. The data are expressed as fold induction with respect to nonstimulated cells.

Immunoblot analysis and electrophoretic mobility shift assays

The following optimal stimulation conditions were used. EBV-B or U3C cells were stimulated by incubation for 20 min with 100 µg/ml IL-21 or 25 ng of IL-22; 30 min with 10^3 or 10^5 IU/ml IFN-γ and IFN-α; 15 min with 50 ng/ml IL-6; or 30 min with 50 or 100 ng/ml IL-27. WB was performed as previously described (Dupuis et al., 2003). In brief, cell activation was blocked with cold 1X PBS, cells were lysed in 1% NP-40 lysis buffer, and the proteins were recovered and subjected to SDS-PAGE. We used antibodies directed against phosphorylated STAT1 (pY701; BD), STAT1 (C-24; Santa Cruz Biotechnology), V5 (Invitrogen), α-tubulin (Santa Cruz Biotechnology), phosphorylated STAT3 (Cell Signaling Technology), lamin B1 (Santa Cruz Biotechnology), GAPDH (Santa Cruz Biotechnology), and STAT3 (Santa Cruz Biotechnology). EMSA was performed as previously described (Chapgier et al., 2006a). In brief, cell activation was blocked by incubation with cold 1X PBS, and the cells were gently lysed to remove cytoplasmic proteins while keeping the nucleus intact. We then added nuclear lysis buffer and recovered the nuclear proteins, which were subjected to nondenaturing electrophoresis with radiolabeled GAS (from the FCγR1 promoter: 5′-ATGTATTTCCCAGAAA-3′) and ISRE (from the ISG15 promoter: 5′-GATCGGGAAAGGGAAACCGAAACTGAA-3′) probes.

Staurosporine and pervanadate treatment of cells

We assessed dephosphorylation by stimulating U3C transfectants with 10^5 IU/ml IFN-γ. The cells were then washed and incubated with 1 µM staurosporine in DME for 15, 30, or 60 min. The cells were then lysed with 1% NP-40 lysis buffer, and the proteins recovered were subjected to immunoblot analysis.

Pervanadate was prepared by mixing orthovanadate with H_2O_2 for 15 min at 22°C. U3C transfectants were treated with pervanadate (0.8 mM orthovanadate and 0.2 mM H_2O_2) 5 min before stimulation. They were then stimulated with IFN-γ for 20 min. The stimulation was stopped by adding cold 1X PBS. The proteins were recovered and subjected to immunoblot analysis.

Extraction of nuclear and cytoplasmic proteins

U3C transfectants or EBV-B cells were stimulated with IFN-γ or IFN-α for 20 min and subjected to nuclear and cytoplasmic protein extraction with NE-PER Nuclear and Cytoplasmic Extraction Regents (Thermo Fisher Scientific) according to the manufacturer's protocol.

Immunofluorescence staining

Immunofluorescence experiments were performed as previously described (Chapgier et al., 2006a). In brief, cells (transfected U3C or SV-40 fibroblasts) were stimulated for the times indicated with 10,000 IU/ml of IFN-γ. Cells were then washed with cold PBS and fixed with 4% PFA. The cells were washed and incubated with an antibody against STAT1, which was then detected by incubation with an Alexa Fluor 488–conjugated anti–mouse antibody.

T cell blast differentiation and stimulation

PBMCs were recovered by centrifuging blood samples on Ficoll gradients, as previously described (Chapgier et al., 2006a). They were then cultivated, at a density of 1 million cells per ml in RPMI supplemented with 10% fetal calf serum and stimulated with phytohemagglutinin (1 µg/ml) for 3 d. Cells were then recovered, centrifuged on a Ficoll gradient, cultivated (at a density of 0.2 million cells/ml) to Panserin 401 supplemented with 10% FCS and glutamine 1X, and stimulated with 40 IU/ml IL-2 (Roche). Cells were then incubated for 30 min with 100 ng/ml IL-23. Activation was stopped by adding 1X cold PBS, and cells were processed for immunoblot analysis.

Modeling

Images of the three-dimensional structure of STAT1 (Chen et al., 1998) were generated with the 2002 PyMOL Molecular Graphics System (DeLano Scientific), using PDB accession no. 1BF5.

Whole-blood assay of the IL-12–IFN-γ circuit

Whole-blood assays were performed as previously described (Feinberg et al., 2004). Heparin-treated blood samples from healthy controls and patients were stimulated in vitro with live *Mycobacterium bovis* BCG (Pasteur) alone or with IFN-γ (5,000 IU/ml; Boehringer Ingelheim). Supernatants were collected after 48 h of stimulation, and ELISA were performed with specific antibodies directed against IL-12p40 or IL-12p70, using kits from R&D Systems according to the manufacturer's instructions.

Production of IL-17A, IL-17F, and IL-22 by leukocytes

Cell activation. IL-17A– and IL-22–producing T cells were evaluated by intracellular staining or by ELISA, as previously described (de Beaucoudrey et al., 2008). In brief, PBMCs were purified by centrifugation on a gradient (Ficoll-Paque PLUS; GE Healthcare) and resuspended in RPMI supplemented with 10% FBS (RPMI/10% FBS; Invitrogen). Adherent monocytes were removed from the PBMC preparation by incubation for 2 h at 37°C, under an atmosphere containing 5% CO_2.

For ex vivo evaluation of IL-17– and IL-22–producing T cells by flow cytometry, we resuspended 5 × 10^6 nonadherent cells in 5 ml RPMI/10% FBS in 25 cm^2 flasks and stimulated them by incubation with 40 ng/ml PMA (Sigma-Aldrich) and 10^{-5} M ionomycin (Sigma-Aldrich) in the presence of a secretion inhibitor (1 µl/ml GolgiPlug; BD) for 12 h.

For evaluation of the IL-17– and IL-22–producing T cell blasts after in vitro differentiation, the nonadherent PBMCs were dispensed into 24-well plates at a density of 2.5 × 10^6 cells/ml in RPMI/10% FBS and activated with 2 µg/ml of an antibody directed against CD3 (Orthoclone OKT3; Janssen-Cilag) alone, or together with 5 ng/ml TGF-β1 (240-B; R&D Systems), 20 ng/ml IL-23 (1290-IL; R&D Systems), 50 ng/ml IL-6 (206-IL; R&D Systems), 10 ng/ml IL-1β (201-LB; R&D Systems), or combinations of these four cytokines. After 3 d, the cells were restimulated in the same activation conditions, except that the anti-CD3 antibody was replaced with 40 IU/ml IL-2 (Proleukin i.v.; Chiron). We added 1 ml of the appropriate medium, resuspended the cells by gentle pipetting, and then split the cell suspension from each well into two. Flow cytometry was performed on one of the duplicated wells 2 d later, after stimulation by incubation for 12 h with 40 ng/ml PMA and 10^{-5} M ionomycin in the presence of 1 µl/ml GolgiPlug. FACS analysis was performed as described in the following section. The other duplicated well was split into two, with one half left unstimulated and the other stimulated by incubation with 40 ng/ml PMA and 10^{-5} M ionomycin for another 2 d. Supernatants were collected after 48 h of incubation, for ELISA.

Flow cytometry. Cells were washed in cold PBS, and surface labeling was achieved by incubating the cells with PECy5-conjugated anti–human CD3 antibody (BD) in PBS/2% FBS for 20 min on ice. Cells were then washed twice with 2% FBS in cold PBS, fixed by incubation with 100 µl of BD Cytofix for 30 min on ice, and washed twice with BD Cytoperm (Cytofix/Cytoperm Plus, fixation/permeabilization kit; BD). Cells were then incubated for 1 h on ice with Alexa Fluor 488–conjugated anti–human IL-17A (53-7179-42; eBioscience), PE-conjugated anti–human IL-22 (IC7821P; R&D Systems), or PE-conjugated anti–human IFN-γ (IC285P; R&D Systems) antibodies, washed twice with Cytoperm, and analyzed with a FACSCanto II system (BD).

ELISA. IL-17A, IL-17F, and IL-22 levels were determined by ELISA on the supernatants harvested after 48 h of whole-blood stimulation with 40 ng/ml PMA and 10^{-5} M ionomycin, or after in vitro PHA blast differentiation and

48 h of stimulation with 40 ng/ml PMA and 10^{-5} M ionomycin. We used anti–human IL-17A and anti–human IL-22 Duoset kits (R&D Systems) and the anti–human IL-17F ELISA Ready-SET-GO! set (eBioscience).

Statistical analysis. We assessed differences between controls, MSMD patients bearing loss-of-function *STAT1* alleles, and CMCD patients bearing gain-of-function *STAT1* alleles in terms of the percentages of IL-17A– and IL-22–producing T cells, as assessed by flow cytometry, and in terms of the amounts of IL-17A, IL-17F, and IL-22 produced in various stimulation conditions, as assessed by ELISA. We used the nonparametric Wilcoxon test, as implemented in the PROC NPAR1WAY of the SAS software version 9.1 (SAS Institute). For all analyses, $P < 0.05$ was considered statistically significant.

Online supplemental material

Fig. S1 shows that STAT1-CMCD mutants are gain-of-function alleles by loss of nuclear dephosphorylation. Fig. S2 is a schematic representation of the cytokines and transcription factors directing the development of naive CD4 cells into IL-17–producing T cells. Fig. S3 shows the normal response of CMCD patient cells to IFN-α in terms of ISGF3 activation, to IFN-γ in terms of STAT1 nuclear translocation; and to IL-23 and IL-22 in terms of pSTAT3. Fig. S4 shows impaired in vitro differntiation of IL-17– and Il-22–producing T cell blasts in patients with CMCD and gain-of-function SATA1 mustations. Table S1 shows novel coding heterozygous variants found by whole-exome sequencing in the 6 different patients. Table S2 shows novel coding heterozygous variants found by whole-exome sequencing within genes shared by more than one patient. Table S3 lists conservation and predictions on the function of the mutant STAT1 alleles associated with CMCD. Table S4 lists the STAT1 GOF mutation created, and the pair of primers used. Online supplemental material is available at http://www.jem.org/cgi/content/full/jem.20110958/DC1.

We thank the members of the laboratory for helpful discussions; Yelena Nemiroskaya, Eric Anderson, Martine Courat, and Michele N'Guyen for secretarial assistance; and Tony Leclerc and Tiffany Nivare for technical assistance. We also thank Alekszandra Barsony, Dmitriy Samarin, Fedir Lapiy, Maxim Vodyanik, Marcela Moncada Velez, Bertrand Boisson, and Astrid Research, Inc.

This work was supported by grants from Institut National de la Santé et de la Recherche Médicale, University Paris Descartes, the Rockefeller University, the Rockefeller University CTSA grant number 5UL1RR024143-04, the St. Giles Foundation, and the Candidoser Association awarded to Jean-Laurent Casanova. Janine Reichenbach was supported by the Gebert Rüf Stiftung, program "Rare Diseases - New Approaches"; Ellen Renner by the DFG RE2799/3-1 and a Fritz-Thyssen research foundation grant (Az. 10.07.1.159). Support was also provided by TÁMOP 4.2.1./B-09/1/KONV-2010-0007 and TÁMOP 4.2.2-08/1-2008-0015 grants to László Maródi and LMU Munich FöFoLe grant #680/658. Sophie Cypowyj was supported by the AXA Research Fund, and Xiaofei Kong by the Choh-Hao Li Memorial Fund Scholar award and the Shanghai Educational Development Foundation. We have all the approvals and authorizations required for this study (Necker IRB, Paris, 1995 and Rockefeller IRB, New York, 2008).

The authors state no conflict of interest.

Submitted: 11 May 2011
Accepted: 22 June 2011

REFERENCES

Adzhubei, I.A., S. Schmidt, L. Peshkin, V.E. Ramensky, A. Gerasimova, P. Bork, A.S. Kondrashov, and S.R. Sunyaev. 2010. A method and server for predicting damaging missense mutations. *Nat. Methods.* 7:248–249. doi:10.1038/nmeth0410-248

Alcaïs, A., L. Abel, and J.L. Casanova. 2009. Human genetics of infectious diseases: between proof of principle and paradigm. *J. Clin. Invest.* 119:2506–2514. doi:10.1172/JCI38111

Alcaïs, A., L. Quintana-Murci, D.S. Thaler, E. Schurr, L. Abel, and J.L. Casanova. 2010. Life-threatening infectious diseases of childhood: single-gene inborn errors of immunity? *Ann. N.Y.Acad. Sci.* 1214:18–33. doi:10.1111/j.1749-6632.2010.05834.x

Amadi-Obi, A., C.R. Yu, X. Liu, R.M. Mahdi, G.L. Clarke, R.B. Nussenblatt, I. Gery, Y.S. Lee, and C.E. Egwuagu. 2007. TH17 cells contribute to uveitis and scleritis and are expanded by IL-2 and inhibited by IL-27/STAT1. *Nat. Med.* 13:711–718. doi:10.1038/nm1585

Atkinson, T.P., A.A. Schäffer, B. Grimbacher, H.W. Schroeder Jr., C. Woellner, C.S. Zerbe, and J.M. Puck. 2001. An immune defect causing dominant chronic mucocutaneous candidiasis and thyroid disease maps to chromosome 2p in a single family. *Am. J. Hum. Genet.* 69:791–803. doi:10.1086/323611

Averbuch, D., A. Chapgier, S. Boisson-Dupuis, J.L. Casanova, and D. Engelhard. 2011. The clinical spectrum of patients with deficiency of Signal Transducer and Activator of Transcription-1. *Pediatr. Infect. Dis. J.* 30:352–355.

Batten, M., J. Li, S. Yi, N.M. Kljavin, D.M. Danilenko, S. Lucas, J. Lee, F.J. de Sauvage, and N. Ghilardi. 2006. Interleukin 27 limits autoimmune encephalomyelitis by suppressing the development of interleukin 17-producing T cells. *Nat. Immunol.* 7:929–936. doi:10.1038/ni1375

Bentur, L., E. Nisbet-Brown, H. Levison, and C.M. Roifman. 1991. Lung disease associated with IgG subclass deficiency in chronic mucocutaneous candidiasis. *J. Pediatr.* 118:82–86. doi:10.1016/S0022-3476(05)81852-9

Bolze, A., M. Byun, D. McDonald, N.V. Morgan, A. Abhyankar, L. Premkumar, A. Puel, C.M. Bacon, F. Rieux-Laucat, K. Pang, et al. 2010. Whole-exome-sequencing-based discovery of human FADD deficiency. *Am. J. Hum. Genet.* 87:873–881. doi:10.1016/j.ajhg.2010.10.028

Braunstein, J., S. Brutsaert, R. Olson, and C. Schindler. 2003. STATs dimerize in the absence of phosphorylation. *J. Biol. Chem.* 278:34133–34140. doi:10.1074/jbc.M304531200

Byun, M., A. Abhyankar, V. Lelarge, S. Plancoulaine, A. Palanduz, L. Telhan, B. Boisson, C. Picard, S. Dewell, C. Zhao, et al. 2010. Whole-exome sequencing-based discovery of STIM1 deficiency in a child with fatal classic Kaposi sarcoma. *J. Exp. Med.* 207:2307–2312. doi:10.1084/jem.20101597

Casanova, J.L., and L. Abel. 2005. Inborn errors of immunity to infection: the rule rather than the exception. *J. Exp. Med.* 202:197–201. doi:10.1084/jem.20050854

Casanova, J.L., and L. Abel. 2007. Primary immunodeficiencies: a field in its infancy. *Science.* 317:617–619. doi:10.1126/science.1142963

Chapgier, A., S. Boisson-Dupuis, E. Jouanguy, G. Vogt, J. Feinberg, A. Prochnicka-Chalufour, A. Casrouge, K. Yang, C. Soudais, C. Fieschi, et al. 2006a. Novel STAT1 alleles in otherwise healthy patients with mycobacterial disease. *PLoS Genet.* 2:e131. doi:10.1371/journal.pgen.0020131

Chapgier, A., R.F. Wynn, E. Jouanguy, O. Filipe-Santos, S. Zhang, J. Feinberg, K. Hawkins, J.L. Casanova, and P.D. Arkwright. 2006b. Human complete Stat-1 deficiency is associated with defective type I and II IFN responses in vitro but immunity to some low virulence viruses in vivo. *J. Immunol.* 176:5078–5083.

Chapgier, A., X.F. Kong, S. Boisson-Dupuis, E. Jouanguy, D. Averbuch, J. Feinberg, S.Y. Zhang, J. Bustamante, G. Vogt, J. Lejeune, et al. 2009. A partial form of recessive STAT1 deficiency in humans. *J. Clin. Invest.* 119:1502–1514. doi:10.1172/JCI37083

Chen, X., U. Vinkemeier, Y. Zhao, D. Jeruzalmi, J.E. Darnell Jr., and J. Kuriyan. 1998. Crystal structure of a tyrosine phosphorylated STAT-1 dimer bound to DNA. *Cell.* 93:827–839. doi:10.1016/S0092-8674(00)81443-9

Chen, M., G. Chen, H. Nie, X. Zhang, X. Niu, Y.C. Zang, S.M. Skinner, J.Z. Zhang, J.M. Killian, and J. Hong. 2009. Regulatory effects of IFN-beta on production of osteopontin and IL-17 by CD4+ T Cells in MS. *Eur. J. Immunol.* 39:2525–2536. doi:10.1002/eji.200838879

Crabé, S., A. Guay-Giroux, A.J. Tormo, D. Duluc, R. Lissilaa, F. Guilhot, U. Mavoungou-Bigouagou, F. Lefouili, I. Cognet, W. Ferlin, et al. 2009. The IL-27 p28 subunit binds cytokine-like factor 1 to form a cytokine regulating NK and T cell activities requiring IL-6R for signaling. *J. Immunol.* 183:7692–7702. doi:10.4049/jimmunol.0901464

de Beaucoudrey, L., A. Puel, O. Filipe-Santos, A. Cobat, P. Ghandil, M. Chrabieh, J. Feinberg, H. von Bernuth, A. Samarina, L. Jannière, et al. 2008. Mutations in STAT3 and IL12RB1 impair the development of human IL-17-producing T cells. *J. Exp. Med.* 205:1543–1550. doi:10.1084/jem.20080321

de Beaucoudrey, L., A. Samarina, J. Bustamante, A. Cobat, S. Boisson-Dupuis, J. Feinberg, S. Al-Muhsen, L. Jannière, Y. Rose, M. de Suremain, et al. 2010. Revisiting human IL-12Rβ1 deficiency: a survey of 141 patients from 30 countries. *Medicine.* 89:381–402. doi:10.1097/MD.0b013e3181fdd832

Diveu, C., M.J. McGeachy, K. Boniface, J.S. Stumhofer, M. Sathe, B. Joyce-Shaikh, Y. Chen, C.M. Tato, T.K. McClanahan, R. de Waal Malefyt, et al. 2009. IL-27 blocks RORc expression to inhibit lineage commitment of Th17 cells. *J. Immunol.* 182:5748–5756. doi:10.4049/jimmunol.0801162

Donnelly, R.P., F. Sheikh, H. Dickensheets, R. Savan, H.A. Young, and M.R. Walter. 2010. Interleukin-26: an IL-10-related cytokine produced by Th17 cells. *Cytokine Growth Factor Rev.* 21:393–401. doi:10.1016/j.cytogfr.2010.09.001

Dupuis, S., C. Dargemont, C. Fieschi, N. Thomassin, S. Rosenzweig, J. Harris, S.M. Holland, R.D. Schreiber, and J.L. Casanova. 2001. Impairment of mycobacterial but not viral immunity by a germline human STAT1 mutation. *Science.* 293:300–303. doi:10.1126/science.1061154

Dupuis, S., E. Jouanguy, S. Al-Hajjar, C. Fieschi, I.Z. Al-Mohsen, S. Al-Jumaah, K. Yang, A. Chapgier, C. Eidenschenk, P. Eid, et al. 2003. Impaired response to interferon-alpha/beta and lethal viral disease in human STAT1 deficiency. *Nat. Genet.* 33:388–391. doi:10.1038/ng1097

El-behi, M., B. Ciric, S. Yu, G.X. Zhang, D.C. Fitzgerald, and A. Rostami. 2009. Differential effect of IL-27 on developing versus committed Th17 cells. *J. Immunol.* 183:4957–4967. doi:10.4049/jimmunol.0900735

Eyerich, K., S. Foerster, S. Rombold, H.P. Seidl, H. Behrendt, H. Hofmann, J. Ring, and C. Traidl-Hoffmann. 2008. Patients with chronic mucocutaneous candidiasis exhibit reduced production of Th17-associated cytokines IL-17 and IL-22. *J. Invest. Dermatol.* 128:2640–2645. doi:10.1038/jid.2008.139

Feinberg, J., C. Fieschi, R. Doffinger, M. Feinberg, T. Leclerc, S. Boisson-Dupuis, C. Picard, J. Bustamante, A. Chapgier, O. Filipe-Santos, et al. 2004. Bacillus Calmette Guerin triggers the IL-12/IFN-gamma axis by an IRAK-4- and NEMO-dependent, non-cognate interaction between monocytes, NK, and T lymphocytes. *Eur. J. Immunol.* 34:3276–3284. doi:10.1002/eji.200425221

Feng, G., W. Gao, T.B. Strom, M. Oukka, R.S. Francis, K.J. Wood, and A. Bushell. 2008. Exogenous IFN-gamma ex vivo shapes the alloreactive T-cell repertoire by inhibition of Th17 responses and generation of functional Foxp3+ regulatory T cells. *Eur. J. Immunol.* 38:2512–2527. doi:10.1002/eji.200838411

Filipe-Santos, O., J. Bustamante, A. Chapgier, G. Vogt, L. de Beaucoudrey, J. Feinberg, E. Jouanguy, S. Boisson-Dupuis, C. Fieschi, C. Picard, and J.L. Casanova. 2006. Inborn errors of IL-12/23- and IFN-gamma-mediated immunity: molecular, cellular, and clinical features. *Semin. Immunol.* 18:347–361. doi:10.1016/j.smim.2006.07.010

Germain, M., M. Gourdeau, and J. Hébert. 1994. Case report: familial chronic mucocutaneous candidiasis complicated by deep candida infection. *Am. J. Med. Sci.* 307:282–283. doi:10.1097/00000441-199404000-00008

Glocker, E.O., A. Hennigs, M. Nabavi, A.A. Schäffer, C. Woellner, U. Salzer, D. Pfeifer, H. Veelken, K. Warnatz, F. Tahami, et al. 2009. A homozygous CARD9 mutation in a family with susceptibility to fungal infections. *N. Engl. J. Med.* 361:1727–1735. doi:10.1056/NEJMoa0810719

Guzzo, C., N.F. Che Mat, and K. Gee. 2010. Interleukin-27 induces a STAT1/3- and NF-kappaB-dependent proinflammatory cytokine profile in human monocytes. *J. Biol. Chem.* 285:24404–24411. doi:10.1074/jbc.M110.112599

Herrod, H.G. 1990. Chronic mucocutaneous candidiasis in childhood and complications of non-Candida infection: a report of the Pediatric Immunodeficiency Collaborative Study Group. *J. Pediatr.* 116:377–382. doi:10.1016/S0022-3476(05)82824-0

Hirahara, K., K. Ghoreschi, A. Laurence, X.P. Yang, Y. Kanno, and J.J. O'Shea. 2010. Signal transduction pathways and transcriptional regulation in Th17 cell differentiation. *Cytokine Growth Factor Rev.* 21:425–434. doi:10.1016/j.cytogfr.2010.10.006

Hoshino, A., S. Saint Fleur, and H. Fujii. 2006. Regulation of Stat1 protein expression by phenylalanine 172 in the coiled-coil domain. *Biochem. Biophys. Res. Commun.* 346:1062–1066. doi:10.1016/j.bbrc.2006.06.026

Hunter, C.A. 2005. New IL-12-family members: IL-23 and IL-27, cytokines with divergent functions. *Nat. Rev. Immunol.* 5:521–531. doi:10.1038/nri1648

Kastelein, R.A., C.A. Hunter, and D.J. Cua. 2007. Discovery and biology of IL-23 and IL-27: related but functionally distinct regulators of inflammation. *Annu. Rev. Immunol.* 25:221–242. doi:10.1146/annurev.immunol.22.012703.104758

Kimura, A., T. Naka, K. Nohara, Y. Fujii-Kuriyama, and T. Kishimoto. 2008. Aryl hydrocarbon receptor regulates Stat1 activation and participates in the development of Th17 cells. *Proc. Natl. Acad. Sci. USA.* 105:9721–9726. doi:10.1073/pnas.0804231105

Kirkpatrick, C.H. 2001. Chronic mucocutaneous candidiasis. *Pediatr. Infect. Dis. J.* 20:197–206. doi:10.1097/00006454-200102000-00017

Kisand, K., A.S. Bøe Wolff, K.T. Podkrajsek, L. Tserel, M. Link, K.V. Kisand, E. Ersvaer, J. Perheentupa, M.M. Erichsen, N. Bratanic, et al. 2010. Chronic mucocutaneous candidiasis in APECED or thymoma patients correlates with autoimmunity to Th17-associated cytokines. *J. Exp. Med.* 207:299–308. doi:10.1084/jem.20091669

Kishimoto, T. 2005. Interleukin-6: from basic science to medicine—40 years in immunology. *Annu. Rev. Immunol.* 23:1–21. doi:10.1146/annurev.immunol.23.021704.115806

Kong, X.F., M. Ciancanelli, S. Al-Hajjar, L. Alsina, T. Zumwalt, J. Bustamante, J. Feinberg, M. Audry, C. Prando, V. Bryant, et al. 2010. A novel form of human STAT1 deficiency impairing early but not late responses to interferons. *Blood.* 116:5895–5906. doi:10.1182/blood-2010-04-280586

Kristensen, I.A., J.E. Veirum, B.K. Møller, and M. Christiansen. 2011. Novel STAT1 Alleles in a Patient with Impaired Resistance to Mycobacteria. *J. Clin. Immunol.* 31:265–271. doi:10.1007/s10875-010-9480-8

Levy, D.E., and J.E. Darnell Jr. 2002. Stats: transcriptional control and biological impact. *Nat. Rev. Mol. Cell Biol.* 3:651–662. doi:10.1038/nrm909

Li, H., and R. Durbin. 2009. Fast and accurate short read alignment with Burrows-Wheeler transform. *Bioinformatics.* 25:1754–1760.

Lilic, D. 2002. New perspectives on the immunology of chronic mucocutaneous candidiasis. *Curr. Opin. Infect. Dis.* 15:143–147. doi:10.1097/00001432-200204000-00007

Liu, H., and C. Rohowsky-Kochan. 2011. Interleukin-27-Mediated Suppression of Human Th17 Cells Is Associated with Activation of STAT1 and Suppressor of Cytokine Signaling Protein 1. *J. Interferon Cytokine Res.* 31:459–469. doi:10.1089/jir.2010.0115

Ma, C.S., G.Y. Chew, N. Simpson, A. Priyadarshi, M. Wong, B. Grimbacher, D.A. Fulcher, S.G. Tangye, and M.C. Cook. 2008. Deficiency of Th17 cells in hyper IgE syndrome due to mutations in STAT3. *J. Exp. Med.* 205:1551–1557. doi:10.1084/jem.20080218

McKenna, A., M. Hanna, E. Banks, A. Sivachenko, K. Cibulskis, A. Kernytsky, K. Garimella, D. Altshuler, S. Gabriel, M. Daly, and M.A. DePristo. 2010. The Genome Analysis Toolkit: a MapReduce framework for analyzing next-generation DNA sequencing data. *Genome Res.* 20:1297–1303.

Mertens, C., M. Zhong, R. Krishnaraj, W. Zou, X. Chen, and J.E. Darnell Jr. 2006. Dephosphorylation of phosphotyrosine on STAT1 dimers requires extensive spatial reorientation of the monomers facilitated by the N-terminal domain. *Genes Dev.* 20:3372–3381. doi:10.1101/gad.1485406

Milner, J.D., J.M. Brenchley, A. Laurence, A.F. Freeman, B.J. Hill, K.M. Elias, Y. Kanno, C. Spalding, H.Z. Elloumi, M.L. Paulson, et al. 2008. Impaired T(H)17 cell differentiation in subjects with autosomal dominant hyper-IgE syndrome. *Nature.* 452:773–776. doi:10.1038/nature06764

Minegishi, Y. 2009. Hyper-IgE syndrome. *Curr. Opin. Immunol.* 21:487–492. doi:10.1016/j.coi.2009.07.013

Minegishi, Y., M. Saito, M. Nagasawa, H. Takada, T. Hara, S. Tsuchiya, K. Agematsu, M. Yamada, N. Kawamura, T. Ariga, et al. 2009. Molecular explanation for the contradiction between systemic Th17 defect and localized bacterial infection in hyper-IgE syndrome. *J. Exp. Med.* 206:1291–1301. doi:10.1084/jem.20082767

Ng, S.B., K.J. Buckingham, C. Lee, A.W. Bigham, H.K. Tabor, K.M. Dent, C.D. Huff, P.T. Shannon, E.W. Jabs, D.A. Nickerson, et al. 2010. Exome sequencing identifies the cause of a mendelian disorder. *Nat. Genet.* 42:30–35. doi:10.1038/ng.499

Oppenheim, Y., Y. Ban, and Y. Tomer. 2004. Interferon induced Autoimmune Thyroid Disease (AITD): a model for human autoimmunity. *Autoimmun. Rev.* 3:388–393. doi:10.1016/j.autrev.2004.03.003

Ouyang, W., S. Rutz, N.K. Crellin, P.A. Valdez, and S.G. Hymowitz. 2011. Regulation and functions of the IL-10 family of cytokines in

Published July 4, 2011

JEM

inflammation and disease. *Annu. Rev. Immunol.* 29:71–109. doi:10.1146/annurev-immunol-031210-101312

Puel, A., R. Döffinger, A. Natividad, M. Chrabieh, G. Barcenas-Morales, C. Picard, A. Cobat, M. Ouachée-Chardin, A. Toulon, J. Bustamante, et al. 2010a. Autoantibodies against IL-17A, IL-17F, and IL-22 in patients with chronic mucocutaneous candidiasis and autoimmune polyendocrine syndrome type I. *J. Exp. Med.* 207:291–297. doi:10.1084/jem.20091983

Puel, A., C. Picard, S. Cypowyj, D. Lilic, L. Abel, and J.L. Casanova. 2010b. Inborn errors of mucocutaneous immunity to Candida albicans in humans: a role for IL-17 cytokines? *Curr. Opin. Immunol.* 22:467–474. doi:10.1016/j.coi.2010.06.009

Puel, A., S. Cypowyj, J. Bustamante, J.F. Wright, L. Liu, H.K. Lim, M. Migaud, L. Israel, M. Chrabieh, M. Audry, et al. 2011. Chronic mucocutaneous candidiasis in humans with inborn errors of interleukin-17 immunity. *Science.* 332:65–68. doi:10.1126/science.1200439

Ramgolam, V.S., Y. Sha, J. Jin, X. Zhang, and S. Markovic-Plese. 2009. IFN-beta inhibits human Th17 cell differentiation. *J. Immunol.* 183:5418–5427. doi:10.4049/jimmunol.0803227

Renner, E.D., S. Rylaarsdam, S. Anover-Sombke, A.L. Rack, J. Reichenbach, J.C. Carey, Q. Zhu, A.F. Jansson, J. Barboza, L.F. Schimke, et al. 2008. Novel signal transducer and activator of transcription 3 (STAT3) mutations, reduced T(H)17 cell numbers, and variably defective STAT3 phosphorylation in hyper-IgE syndrome. *J. Allergy Clin. Immunol.* 122:181–187. doi:10.1016/j.jaci.2008.04.037

Sabat, R. 2010. IL-10 family of cytokines. *Cytokine Growth Factor Rev.* 21:315–324. doi:10.1016/j.cytogfr.2010.11.001

Selmi, C., A. Lleo, M. Zuin, M. Podda, L. Rossaro, and M.E. Gershwin. 2006. Interferon alpha and its contribution to autoimmunity. *Curr. Opin. Investig. Drugs.* 7:451–456.

Shama, S.K., and C.H. Kirkpatrick. 1980. Dermatophytosis in patients with chronic mucocutaneous candidiasis. *J. Am. Acad. Dermatol.* 2:285–294. doi:10.1016/S0190-9622(80)80040-5

Spolski, R., and W.J. Leonard. 2008. Interleukin-21: basic biology and implications for cancer and autoimmunity. *Annu. Rev. Immunol.* 26:57–79. doi:10.1146/annurev.immunol.26.021607.090316

Stumhofer, J.S., A. Laurence, E.H. Wilson, E. Huang, C.M. Tato, L.M. Johnson, A.V. Villarino, Q. Huang, A. Yoshimura, D. Sehy, et al. 2006. Interleukin 27 negatively regulates the development of interleukin 17-producing T helper cells during chronic inflammation of the central nervous system. *Nat. Immunol.* 7:937–945. doi:10.1038/ni1376

Tanaka, K., K. Ichiyama, M. Hashimoto, H. Yoshida, T. Takimoto, G. Takaesu, T. Torisu, T. Hanada, H. Yasukawa, S. Fukuyama, et al. 2008. Loss of suppressor of cytokine signaling 1 in helper T cells leads to defective Th17 differentiation by enhancing antagonistic effects of IFN-gamma on STAT3 and Smads. *J. Immunol.* 180:3746–3756.

Villarino, A.V., E. Gallo, and A.K. Abbas. 2010. STAT1-activating cytokines limit Th17 responses through both T-bet-dependent and -independent mechanisms. *J. Immunol.* 185:6461–6471. doi:10.4049/jimmunol.1001343

Yoshimura, T., A. Takeda, S. Hamano, Y. Miyazaki, I. Kinjyo, T. Ishibashi, A. Yoshimura, and H. Yoshida. 2006. Two-sided roles of IL-27: induction of Th1 differentiation on naive CD4+ T cells versus suppression of proinflammatory cytokine production including IL-23-induced IL-17 on activated CD4+ T cells partially through STAT3-dependent mechanism. *J. Immunol.* 177:5377–5385.

Zhong, M., M.A. Henriksen, K. Takeuchi, O. Schaefer, B. Liu, J. ten Hoeve, Z. Ren, X. Mao, X. Chen, K. Shuai, and J.E. Darnell Jr. 2005. Implications of an antiparallel dimeric structure of nonphosphorylated STAT1 for the activation-inactivation cycle. *Proc. Natl. Acad. Sci. USA.* 102:3966–3971. doi:10.1073/pnas.0501063102

Leukemia Research xxx (2011) xxx–xxx

Contents lists available at ScienceDirect

Leukemia Research

journal homepage: www.elsevier.com/locate/leukres

Genetic analysis of *TP53* in childhood myelodysplastic syndrome and juvenile myelomonocytic leukemia

Shoji Saito[a], Kazuyuki Matsuda[b], Chiaki Taira[b], Kenji Sano[b], Miyuki Tanaka-Yanagisawa[a], Ryu Yanagisawa[a], Yozo Nakazawa[a], Kazuo Sakashita[a], Masaaki Shiohara[a], Kenichi Koike[a,*]

[a] *Department of Pediatrics, Shinshu University School of Medicine, 3-1-1, Asahi, Matsumoto 390-8621, Japan*
[b] *Department of Laboratory Medicine, Shinshu University Hospital, Matsumoto, Japan*

ARTICLE INFO

Article history:
Received 12 April 2011
Received in revised form 16 June 2011
Accepted 22 June 2011
Available online xxx

Keywords:
MDS
JMML
TP53
Childhood
Clone
Biallelic inactivation
MLL duplication

ABSTRACT

Among 9 children with myelodysplastic syndrome (MDS) and 18 children with juvenile myelomonocytic leukemia, one MDS patient with der(5;17)(p10;q10) exhibited deletion of the *TP53* gene in one allele and mutation (410 T>A) in the other allele in myeloid and erythroid cells. Since the mutation was not detected in peripheral blood leukocytes 9 months before the diagnosis, biallelic somatic inactivation of the *TP53* gene might play an important role in the occurrence of MDS. His poor outcome might be associated with resistance to chemotherapy/radiation of a minor clone with both *TP53* gene alteration and *MLL* duplication that already existed at onset.

1. Introduction

The tumor suppressor gene, *TP53*, located on the short arm of chromosome 17 (17p13.1 band), encodes a 53-kDa nuclear phosphoprotein that functions as a negative regulator of cell proliferation. Several types of DNA damage such as those due to certain anticancer drugs and gamma radiation activate the p53 protein, resulting in p53-dependent cell cycle arrest at the G1 and G2 cell cycle checkpoints, allowing time for DNA repair. If the DNA is not repaired, the p53-dependent apoptotic pathway is activated.

Inactivation of p53 has been reported in hematologic malignancies in association with progression of disease. In adult patients with *de novo* myelodysplastic syndrome (MDS) or acute myeloid leukemia (AML), somatically acquired mutations of *TP53* are observed in less than 10% of cases, and are often associated with loss of the short arm of chromosome 17, a complex karyotype, resistance to chemotherapy, and a short survival [1–5].

There has been controversy regarding the frequency of pediatric hematologic malignancies with the *TP53* abnormalities. Felix et al. [6] demonstrated that only one patient showed an inherited 2-base-pair deletion in exon 6 of the *TP53* gene among 19 children with therapy-related leukemia or MDS. On the other hand, Silveira et al. [7] reported that, in a total of 19 pediatric MDS patients including 6 patients who possessed deletion involving 17p13.1, 18 children (94.7%) had deletion of the *TP53* gene according to FISH analysis.

It has been demonstrated that patients with juvenile myelomonocytic leukemia (JMML) have mutually exclusive abnormalities in the GM-CSF signaling pathway (inactivation of the *NF1* tumor suppressor gene or aberrations in *NRAS*, *KRAS*, *PTPN11*, or *CBL* genes) [8,9]. Recently, Sugimoto et al. [10] sequenced exon 12 of ASLX1 in 49 JMML patients, and found 2 novel heterozygous mutations, one occurring as a sole lesion, the other was in conjunction with a PTPN11 mutation. It remains unclear whether the *TP53* abnormalities are observed in JMML patients with genetic abnormalities in the GM-CSF signaling pathway.

In the present study, we examined the presence of *TP53* mutations and deletions in 9 children with MDS or AML with myelodysplasia-related changes and 18 children with JMML by means of DNA sequence, FISH, and immunocytochemical analyses.

2. Materials and methods

The study was approved by the Institutional Review Board of Shinshu University School of Medicine. Informed consent was obtained from parents and patients over 12 years of age.

* Corresponding author. Tel.: +81 263 37 2640; fax: +81 263 37 3089.
E-mail address: koikeken@shinshu-u.ac.jp (K. Koike).

0145-2126/$ – see front matter © 2011 Elsevier Ltd. All rights reserved.
doi:10.1016/j.leukres.2011.06.027

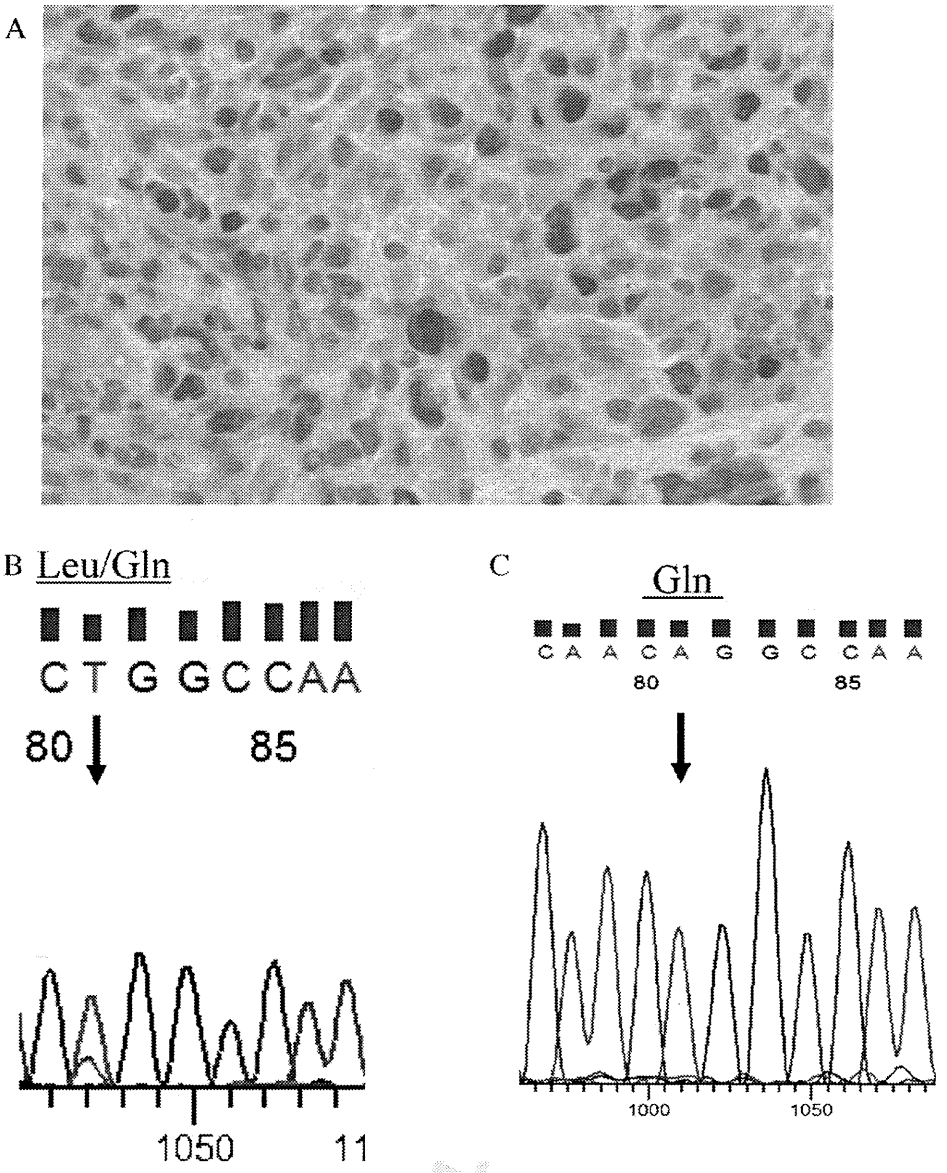

Fig. 1. Immunocytochemical staining for p53 and direct sequencing analysis of TP53 gene at diagnosis in patient no. 6. (A) Paraffin-embedded BM section. Approximately 20% of BM cells were positive for p53. (B and C) The direct sequencing traces showing exon 5 of TP53 gene in circulating mononuclear and CD14+/CD15+ cells. The heterozygous missense mutation was observed in PB mononuclear cells, whereas the homozygous mutation was observed in CD14+/CD15+ PB cells.

2.1. Isolation of bone marrow (BM) and peripheral blood (PB) mononuclear cells

A total of 9 MDS patients and 18 JMML patients, whose clinico-histopathologic features met the World Health Organization diagnostic criteria [11], were enrolled in this study. BM or PB mononuclear cells were separated and frozen with liquid nitrogen until the experiment.

2.2. Detection of TP53 mutations

Exons 5–9 of *TP53* were amplified by polymerase chain reaction (PCR) using the following primers: exons 5–6: sense, 5′-GTTTCTTTGCTGCCGTCTTC-3′; antisense, 5′-CTTAACCCCTCCTCCCAGAG-3′; exon 7: sense, 5′-CTTGCCACAGGTCTCCCCAA-3′; antisense, 5′-AGGGGTCAGAGGCAAGCAGA-3′; exons 7–8: sense, 5′-CTTGGGCCTGTGTTATCTCC-3′; antisense, 5′-TGCTAGGAAAGAGGCAAGGA-3′; exons 8–9: sense, 5′-TTGGGAGTAGATGGAGCCT-3′; antisense, 5′-AGTGTTAGACTGGAAACTTT-3′. The PCR products were subjected to direct sequencing in both directions on an automatic DNA sequencer (ABI Prism 3100 Genetic Analyzer, Applied Biosystems, Foster City, CA) according to the procedure described previously [5]. Mutational analyses of *NRAS, KRAS, PTPN11, CBL, FMS-like tyrosine kinase-3 receptor, c-kit, CSF1R, BRAF, IDH1, and IDH2* genes were performed using primers described previously [9,12–20].

2.3. Immunohistochemical analysis

Reactions with mouse monoclonal anti-p53 antibody (NCL-p53 DO-7; Novocastra, Newcastle upon Tyne, UK) were detected using the Ventana BenchMark LT (Ventana Medical System Inc., AZ) according to the manufacturer's recommendations. The cut-off value was defined as the mean + 2 S.D. obtained from PB cells of normal controls.

2.4. Fluorescence in situ hybridization (FISH) analysis

FISH analysis was performed according to a procedure described previously [21]. We obtained probes specific for the *TP53* (LSI p53 Spectrum Orange Probe), *MLL* (LSI MLL Dual Color, Break Apart Rearrangement Probe), *PML*, and *RARα* genes (PML/RARα Dual Color, Dual Fusion Translocation Probe) from Vysis (Abbott/Vysis, Downers Grove, IL). At least 100 nuclei were scored for the number of hybridization signals of all the genes except for the *MLL* gene in GM or erythroid colony-constituent

Please cite this article in press as: Saito S, et al. Genetic analysis of *TP53* in childhood myelodysplastic syndrome and juvenile myelomonocytic leukemia. Leuk Res (2011), doi:10.1016/j.leukres.2011.06.027